

RADIATIVE TAIL FOR THE PROCESS

$pp \rightarrow \pi^+ d$ NEAR THRESHOLD

by

SEIICHI TANAKA

B.Sc., Saitama University, 1970

A THESIS SUBMITTED IN PARTIAL FULFILLMENT

OF THE REQUIREMENTS FOR THE DEGREE OF

MASTER OF SCIENCE

in the Department

of

Physics

ACCEPTED

We accept this thesis as conforming
to the required standard

Supervisor: Dr. Charles Picciotto

ABSTRACT

A calculation of the radiative tail for the process proton + proton \rightarrow pion + deuteron ($pp \rightarrow \pi d$) is presented. A soft-photon technique is applied in which the radiative amplitude is expressed in terms of the elastic amplitude. Numerical calculations are carried out for incident proton energies of 300 - 400 MeV and pion angles of 1° , 20° and 40° . These values are relevant to proposed experiments which will examine the process proton + proton \rightarrow pion + neutron + proton with very high resolution. This process might be smeared out by the radiative tail of the reaction proton + proton \rightarrow pion + deuteron ($pp \rightarrow \pi d$), and therefore it is important to estimate the contribution from the radiative tail to the pion spectrum. It is found that the radiative tail is very small at the experimental parameters of interest, and therefore one need not worry about this contamination when performing the experiments.




TABLE OF CONTENTS

	<u>Page</u>
ABSTRACT	ii
LIST OF FIGURES	iv
ACKNOWLEDGMENTS	vii
CHAPTER 1 INTRODUCTION	1
CHAPTER 2 GENERAL DISCUSSION OF RADIATIVE CORRECTIONS	7
CHAPTER 3 KINEMATICS FOR THE PROCESSES $pp \rightarrow \pi d$, $pp \rightarrow \pi pn$ AND $pp \rightarrow \pi d \gamma$	14
CHAPTER 4 GENERAL FEYNMAN RULES FOR A CHARGED PARTICLE	28
CHAPTER 5 SOFT-PHOTON THEOREM AND APPLICATION TO SPINLESS CHARGED-PARTICLE SCATTERING	38
CHAPTER 6 CROSS SECTION FOR $pp \rightarrow \pi^+ d \gamma$	44
CHAPTER 7 NUMERICAL CALCULATION AND DISCUSSION	49
REFERENCES	64
APPENDIX A FOUR-COORDINATES AND MOMENTA	66
APPENDIX B THE \mathcal{Y} MATRICES	68
APPENDIX C COMPUTER PROGRAM	69

LIST OF FIGURES

		<u>Page</u>
FIGURE 1.1	Pion energy spectrum for 600 MeV protons at a pion angle of 1°	2
FIGURE 1.2	Pion spectrum as it would appear with high resolution, showing all possible contributions (not in scale)	4
FIGURE 2.1	Typical diagrams containing " virtual " photons	10
FIGURE 2.2	Diagram for elastic electron scattering with exchange of a virtual photon transferring zero energy	10
FIGURE 2.3	Typical diagram containing a " real " photon	10
FIGURE 2.4	A discrete inelastic level, appearing as a bump on the radiative tail of another inelastic peak	13
FIGURE 3.1	Phase space of three- and two-particle final states in the pion spectrum	16
FIGURE 3.2	Pion spectrum for two- and three-particle final states with high resolution showing the possible 1S_0 peak	17
FIGURE 3.3	Expected radiative tail from the process $pp \rightarrow \pi d$	19
FIGURE 3.4	Three-dimensional Laboratory kinematics	21
FIGURE 4.1a	Photon-nucleon vertex	37

	<u>Page</u>
FIGURE 4.1b Photon-pion vertex	37
FIGURE 5.1a Photon emission from external particles	42
FIGURE 5.1b Photon emission from internal particles	42
FIGURE 7.1 Radiative tail from the process $pp \rightarrow \pi^+d$ for 300 MeV protons at a pion angle of 1° . The arrow shows the position of the deuteron peak	52
FIGURE 7.2 Radiative tail from the process $pp \rightarrow \pi^+d$ for 300 MeV protons at a pion angle of 20°	53
FIGURE 7.3 Radiative tail from the process $pp \rightarrow \pi^+d$ for 300 MeV protons at a pion angle of 40°	54
FIGURE 7.4 Radiative tail from the process $pp \rightarrow \pi^+d$ for 350 MeV protons at a pion angle of 1°	55
FIGURE 7.5 Radiative tail from the process $pp \rightarrow \pi^+d$ for 350 MeV protons at a pion angle of 20°	56
FIGURE 7.6 Radiative tail from the process $pp \rightarrow \pi^+d$ for 350 MeV protons at a pion angle of 40°	57
FIGURE 7.7 Radiative tail from the process $pp \rightarrow \pi^+d$ for 400 MeV protons at a pion angle of 1°	58
FIGURE 7.8 Radiative tail from the process $pp \rightarrow \pi^+d$ for 400 MeV protons at a pion angle of 20°	59

ACKNOWLEDGMENTSPage

FIGURE 7.9	Radiative tail from the process pp \rightarrow π^+d for 400 MeV protons at a pion angle of 40°	60
FIGURE 7.10	Radiative tail from the process pp \rightarrow π^+d for 600 MeV protons at a pion angle of 1°	61
FIGURE 7.11	Radiative tail from the process pp \rightarrow π^+d for 600 MeV protons at a pion angle of 20°	62
FIGURE 7.12	Radiative tail from the process pp \rightarrow π^+d for 600 MeV protons at a pion angle of 40°	63

ACKNOWLEDGMENTS

The author is pleased to thank Dr. Charles Picciotto for his guidance in this work.

The author is also grateful to the University of Victoria for their support in the form of a scholarship and fellowship.

CHAPTER 1INTRODUCTION

In recent years the process nucleon + nucleon \rightarrow nucleon + nucleon + pion ($NN \rightarrow NN\pi$) has received much theoretical attention, earlier in the form of multi-parameter calculations (Mandelstam 1958) and more recently in applications of soft-pion techniques (Schillaci et al 1968) and isobar models (Drecshel and Weber 1970). On the experimental side, for the case proton + proton \rightarrow proton + neutron + pi plus ($pp \rightarrow pn\pi^+$) the resolution of the proton beam has not been sufficiently high to separate the deuteron peak entirely from the pn final state in the pion spectrum; a typical spectrum at fixed pion angle is shown in Figure (1.1) (Hirt et al 1969).

With the development of the meson laboratories and their well-defined incident beams, it will be possible to look at this reaction with a pion energy resolution of the order of 1 MeV. In particular, such a proposal has been made at the TRIUMF facility to study π^+ production near threshold. The TRIUMF meson facility is a project

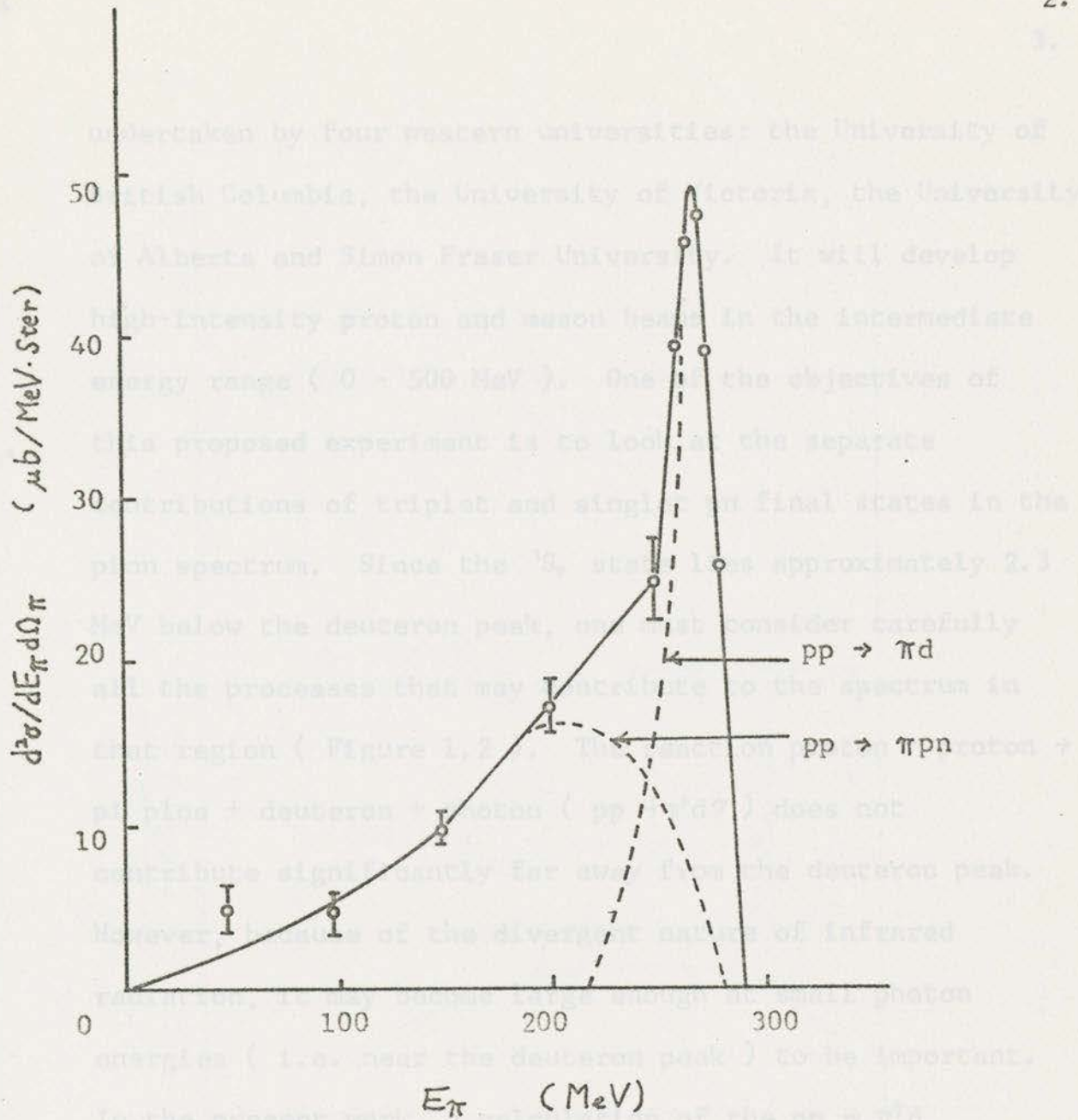


Figure 1.1 Pion energy spectrum for 600 MeV protons at a pion angle of 1°

undertaken by four western universities: the University of British Columbia, the University of Victoria, the University of Alberta and Simon Fraser University. It will develop high-intensity proton and meson beams in the intermediate energy range (0 - 500 MeV). One of the objectives of this proposed experiment is to look at the separate contributions of triplet and singlet pn final states in the pion spectrum. Since the 1S_0 state lies approximately 2.3 MeV below the deuteron peak, one must consider carefully all the processes that may contribute to the spectrum in that region (Figure 1.2). The reaction proton + proton \rightarrow pi plus + deuteron + photon ($pp \rightarrow \pi^+ d \gamma$) does not contribute significantly far away from the deuteron peak. However, because of the divergent nature of infrared radiation, it may become large enough at small photon energies (i.e. near the deuteron peak) to be important. In the present work, a calculation of the $pp \rightarrow \pi^+ d$ radiative tail is presented and estimates of these corrections are obtained. The calculation is carried out with soft-photon techniques, since only the photons of very low energy are considered (Low 1958).

Essentially the soft-photon approximation makes use

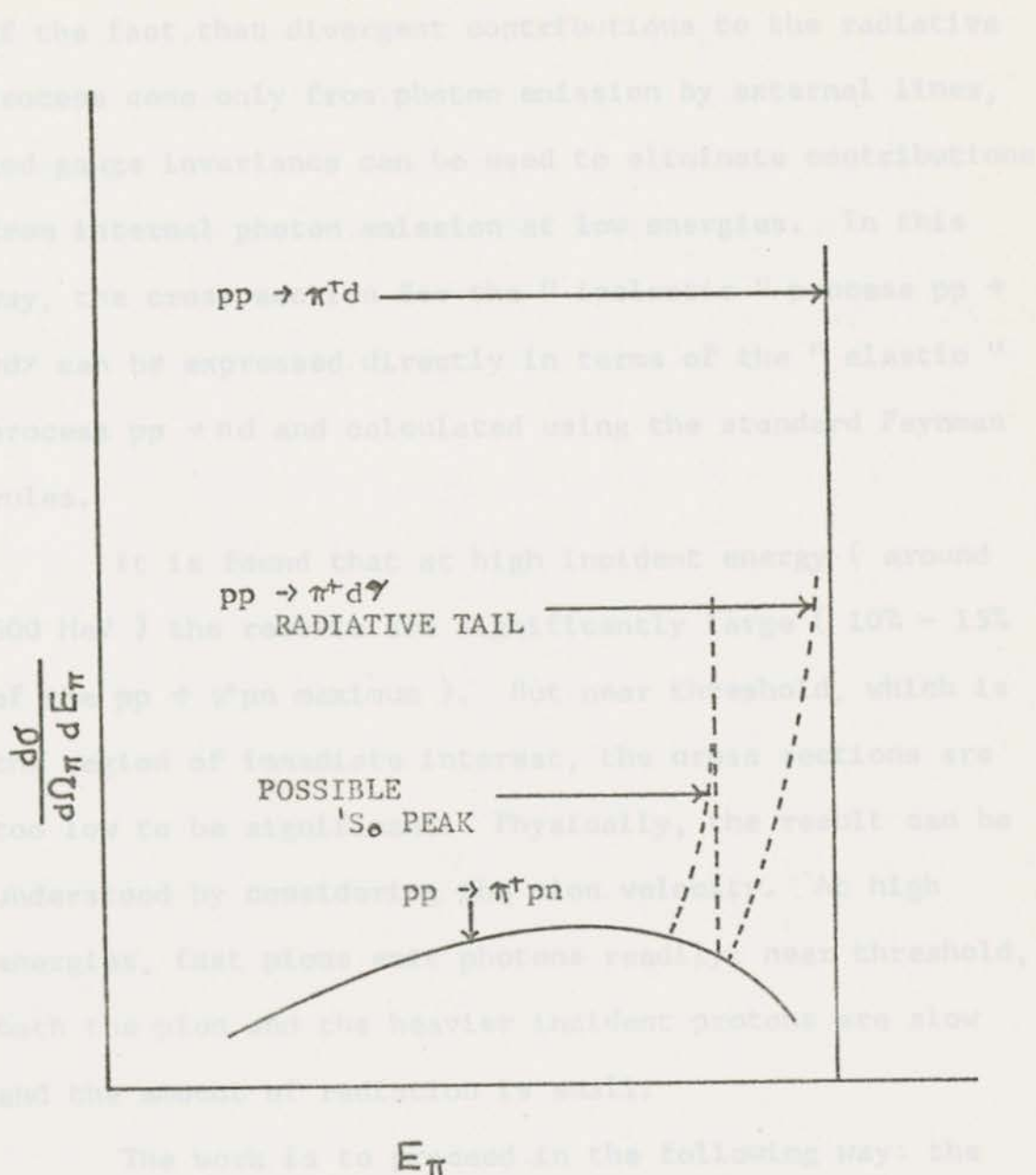


Figure 1.2 Pion spectrum as it would appear with high resolution, showing all possible contributions (not in scale). As derived in the fifth chapter, the soft-photon

of the fact that divergent contributions to the radiative process come only from photon emission by external lines, and gauge invariance can be used to eliminate contributions from internal photon emission at low energies. In this way, the cross section for the "inelastic" process $pp \rightarrow \pi d \gamma$ can be expressed directly in terms of the "elastic" process $pp \rightarrow \pi d$ and calculated using the standard Feynman rules.

It is found that at high incident energy (around 600 MeV) the results are significantly large (10% - 15% of the $pp \rightarrow \pi^+pn$ maximum). But near threshold, which is the region of immediate interest, the cross sections are too low to be significant. Physically, the result can be understood by considering the pion velocity. At high energies, fast pions emit photons readily; near threshold, both the pion and the heavier incident protons are slow and the amount of radiation is small.

The work is to proceed in the following way: the second chapter deals with the general problem of radiative corrections; in the third chapter, the kinematics of the problem are discussed; in the fourth chapter, the Feynman rules are derived; in the fifth chapter, the soft-photon

theorem is presented; in the sixth chapter, the cross section for $pp \rightarrow \pi^+ d \gamma$ is calculated; finally, in the seventh chapter, the numerical calculation is presented followed by a general discussion of the results.

particles is particularly useful because the electromagnetic interaction is well known and is given accurately by quantum-electrodynamics. On the other hand, the propensity for the charged particles to radiate when in the presence of nuclei and other charges makes the analysis of the scattering experiments rather difficult. The radiative background is especially important when the resolution and overall precision of the experiments is high.

Since electrons are relatively light, they radiate readily, and therefore the problem of radiative corrections was first approached in the context of electron scattering. The first calculation of the radiative background to electron scattering was performed by Schwinger in 1949. He dealt with electrons scattered by a point Coulomb potential. In the calculation, he treated the electron-potential field and electron-radiation field interactions to first order and neglected any effect due to recoil of the target (Akhiezer and Berestetskii 1965). Some errors in

CHAPTER 2GENERAL DISCUSSION OF RADIATIVE CORRECTION

The study of nuclear structure with charged particles is particularly useful because the electromagnetic interaction is well known and is given accurately by quantum-electrodynamics. On the other hand, the propensity for the charged particles to radiate when in the presence of nuclei and other charges makes the analysis of the scattering experiments rather difficult. The radiative background is especially important when the resolution and overall precision of the experiments is high.

Since electrons are relatively light, they radiate readily, and therefore the problem of radiative corrections was first approached in the context of electron scattering. The first calculation of the radiative background to electron scattering was performed by Schwinger in 1949. He dealt with electrons scattered by a point Coulomb potential. In the calculation, he treated the electron-potential field and electron-radiation field interactions to first order and neglected any effect due to recoil of the target (Akhiezer and Berestetskii 1965). Some errors in

Schwinger's paper were pointed out by Elton and Robertson (1952) and Motz et al (1964). Many generalization to Schwinger's problem were made (Maximom 1969) to treat various other physical situations.

In the radiative background, one should distinguish the process in which either the charged particles ionize another target atom (Landau straggling) or radiate in the field of another nucleus, from the process in which the charged particle radiates in the field of the same scattering nucleus. The former contribution can be reduced in relative importance by use of thin targets. The latter process, consisting of the proper radiative correction and radiative tail, is more firmly attached to the basic scattering event.

In any discussion of radiative corrections, one often meets terms such as " virtual photon ", " real photon ", " radiative correction " and " radiative tail ". A virtual photon is a photon corresponding to diagrams such as shown in Figure (2.1), i.e. process in which the photon is not a real particle, but is instead exchanged internally by the charged particles that undergo the interactions. The important character of the virtual

photon from the theoretical standpoint is that the square of the four-momentum is not zero, or the mass of the virtual photon is not zero. For example, for elastic electron scattering, in which the virtual photon transfers no energy, the square of the four momentum is

$$\omega^2 - q^2 = (\epsilon_1 - \epsilon_2)^2 - (\vec{p}_1 - \vec{p}_2)^2$$

$$= - (\vec{p}_1 - \vec{p}_2)^2 < 0 ,$$

where ϵ_1, ϵ_2 are the energies of the incident electron and the scattered electron respectively, and \vec{p}_1, \vec{p}_2 are the momenta of the incident electron and the scattered electron respectively (Figure 2.2)

A real photon is a photon corresponding to processes in which there is a real external photon taking part in the interaction and the square of the four momentum is zero, or the mass of the real photon is zero (Figure 2.3).

The distinction between " radiative correction " and " radiative tail " is somewhat arbitrary. The two which will be discussed presently are often called " radiative corrections ". There is, however, a useful distinction both from the experimental and theoretical points of view.

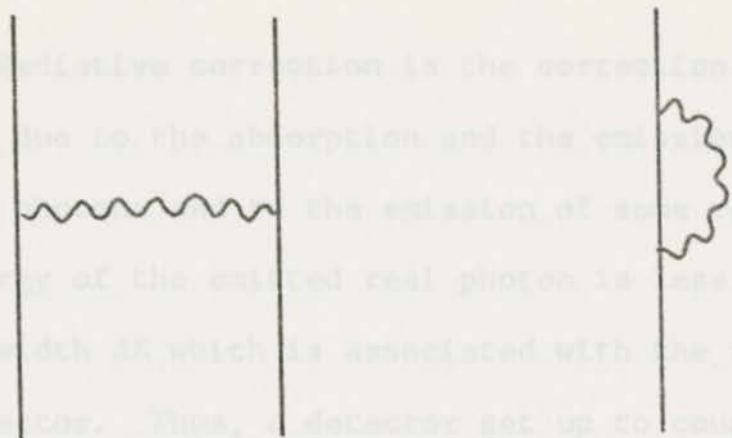


Figure 2.1 Typical diagrams containing " virtual " photons

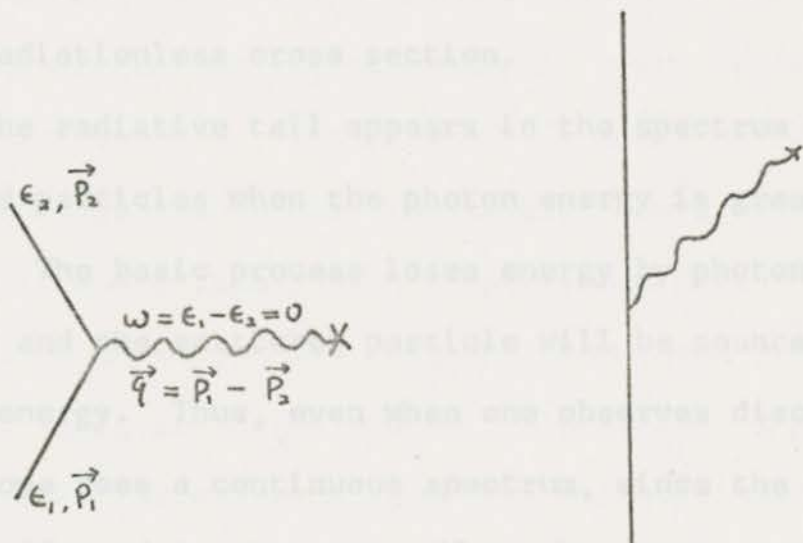


Figure 2.2 Diagram for elastic electron scattering with exchange of a virtual photon transferring zero energy

Figure 2.3 Typical diagram containing a " real " photon

Radiative correction is the correction to the basic process due to the absorption and the emission of the virtual photons and to the emission of some real photons. The energy of the emitted real photon is less than some energy width ΔE which is associated with the resolution of the detector. Thus, a detector set up to count radiationless scattering events will still count an event in which radiation occurred, since the energy carried away by the photon is too small to keep the event from being counted. One must then correct the data in order to exclude all these "inelastic" events and obtain a realistic measure of the radiationless cross section.

The radiative tail appears in the spectrum of scattered particles when the photon energy is greater than ΔE . The basic process loses energy by photon emission and the scattered particle will be counted at a lower energy. Thus, even when one observes discrete states, one sees a continuous spectrum, since the peaks will be affected in this way. When the energy spectrum of the scattered particle consists of several peaks, the radiative tail appears as a background coming from radiative processes involving other states.

As an example, for the case of electron-nucleus scattering, the electron can be scattered elastically or may excite the nucleus to higher energy states. The excited states will appear as peaks in the electron energy spectrum. The peaks would show up clearly in a high-precision experiment, where the spectrometer width ΔE is small. However, they would appear with a background (radiative tail) from processes in which another excited state was created and a photon also given off (Figure 2.4). Thus, one would have to calculate all radiative corrections for each peak (Maximon 1969).

The process $pp \rightarrow \pi^+pn$ presently being treated has a very similar problem. The unbound 1S_0 state of the pn system can appear as a peak in the pion energy spectrum. However, it would appear with a background from the radiative process $pp \rightarrow \pi d\gamma$, where d (deuteron) is a bound 3S_1 state of the pn system. Since this 1S_0 peak is very close to the deuteron peak, the radiative background may be very large. To obtain a proper understanding of the situation it is necessary, therefore, to calculate this radiation tail and estimate its relative importance.

CHAPTER 3

KINEMATICS FOR THE PROCESS $pp \rightarrow \pi^+ d$

$pp \rightarrow \pi^+ n + p$

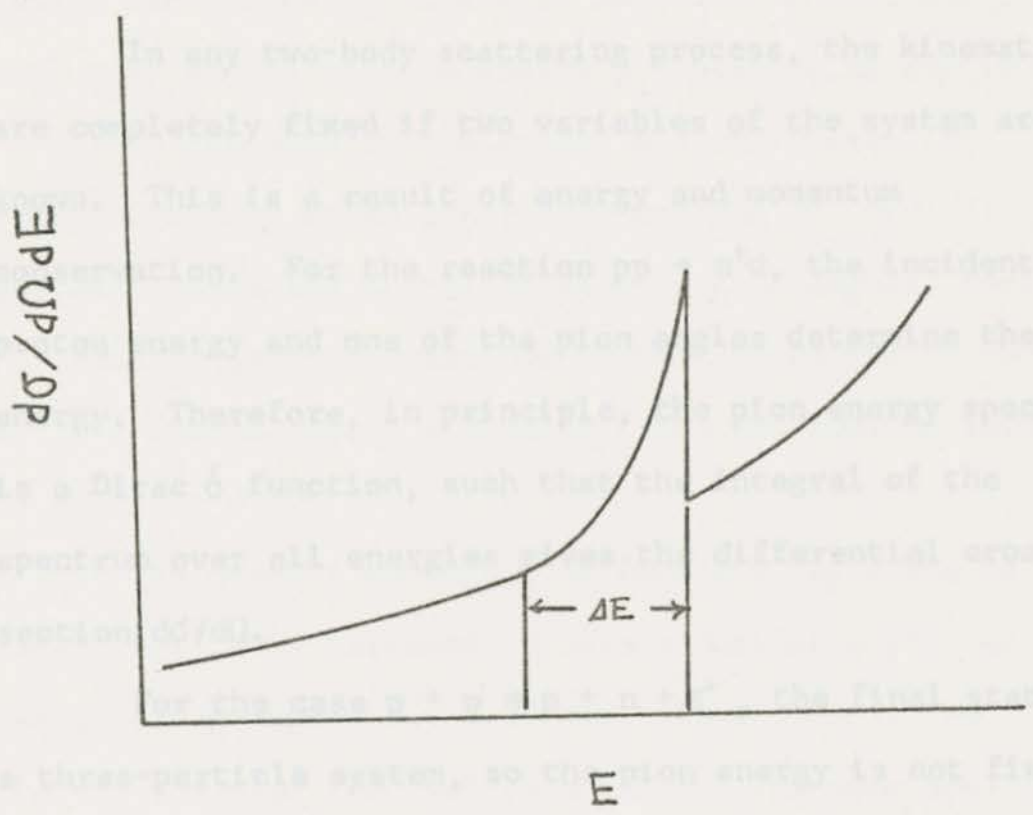


Figure 2.4 A discrete inelastic level, appearing as a bump on the radiative tail of another inelastic peak

CHAPTER 3

KINEMATICS FOR THE PROCESSES $pp \rightarrow \pi d$,

$pp \rightarrow \pi pn$ AND $pp \rightarrow \pi d\gamma$

In any two-body scattering process, the kinematics are completely fixed if two variables of the system are known. This is a result of energy and momentum conservation. For the reaction $pp \rightarrow \pi^+d$, the incident proton energy and one of the pion angles determine the pion energy. Therefore, in principle, the pion energy spectrum is a Dirac δ function, such that the integral of the spectrum over all energies gives the differential cross section $d\sigma/d\Omega$.

For the case $p + p \rightarrow p + n + \pi^+$, the final state is a three-particle system, so the pion energy is not fixed by the pion angle. Instead, a range of energies is allowed, between zero and ξ_{\max} . The maximum energy, ξ_{\max} , is obtained when the proton and neutron come out with the same momentum and the same direction (i.e. as a single particle of mass $2m$, where m is the nucleon mass). Since the binding energy of the deuteron is 2.23 MeV, ξ_{\max} falls approximately 2.23 MeV below the deuteron peak (Figure

3.1). The process will be strongly influenced by the final-state interaction between proton and neutron. Since a high pion energy means a low relative proton-neutron energy and viceversa, the pion spectrum is influenced at the upper end by the low energy p-n scattering amplitude.

In the case of low energy p-n scattering the dominant states which contribute are the 3S_1 and 1S_0 states. These are states of zero orbital angular momentum, 3S_1 being a triplet (the two nucleon spins add to give $s = 1$) and 1S_0 being a singlet (the two nucleon spins add to give $s = 0$).

The overall contribution from the 1S_0 state is very small, but it is believed to have a peak at a p-n relative energy of approximately 0.07 MeV (Paul 1969). We therefore expect the peak to appear in the pion spectrum at approximately 3 MeV below the deuteron peak (Figure 3.2).

On the other hand, the 3S_1 interaction is responsible for the deuteron state, and thus deforms the pion spectrum also at the higher-energy end. Thus, we see that the pion spectrum is primarily composed of two parts, one from the $d + \pi^+$ process and the other from the $p + n + \pi^+$

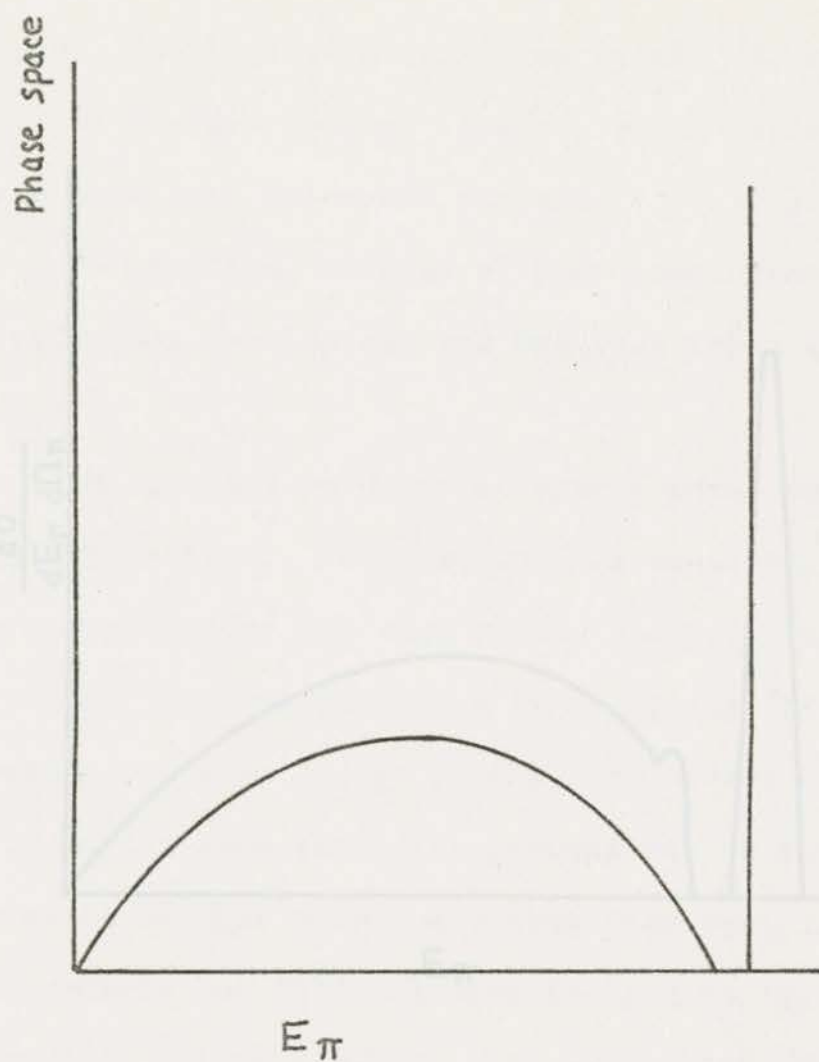


Figure 3.2 Pion spectrum for two- and three- particle

Figure 3.1 Phase space of three- and two-particle final states in the pion spectrum

process. The latter is dominated by the 1S_0 and 3S_1 states of the p-n system. The 3S_1 state is believed to have a peak just below the deuteron (3S_1) peak.

In practice, because of poor resolution both contributions overlap and the spectrum looks as in Figure (3.1).

The process $pp \rightarrow \pi d \gamma$ is also a three-particle final state interaction. However, in this case the maximum pion energy occurs for zero photon energy. In that case, the kinematics correspond to a two-particle final state and therefore the pion energy is the same as for the deuteron peak. At the same time, the process has an infrared divergence at that point, and then dies very quickly with photon energy, so that its contribution to the spectrum is as shown in Figure (3.2). An evaluation of the cross section for $pp \rightarrow \pi d \gamma$ will thus tell us whether or not this process should be taken into account when looking at $pp \rightarrow \pi pn$ with high resolution near the upper end of the

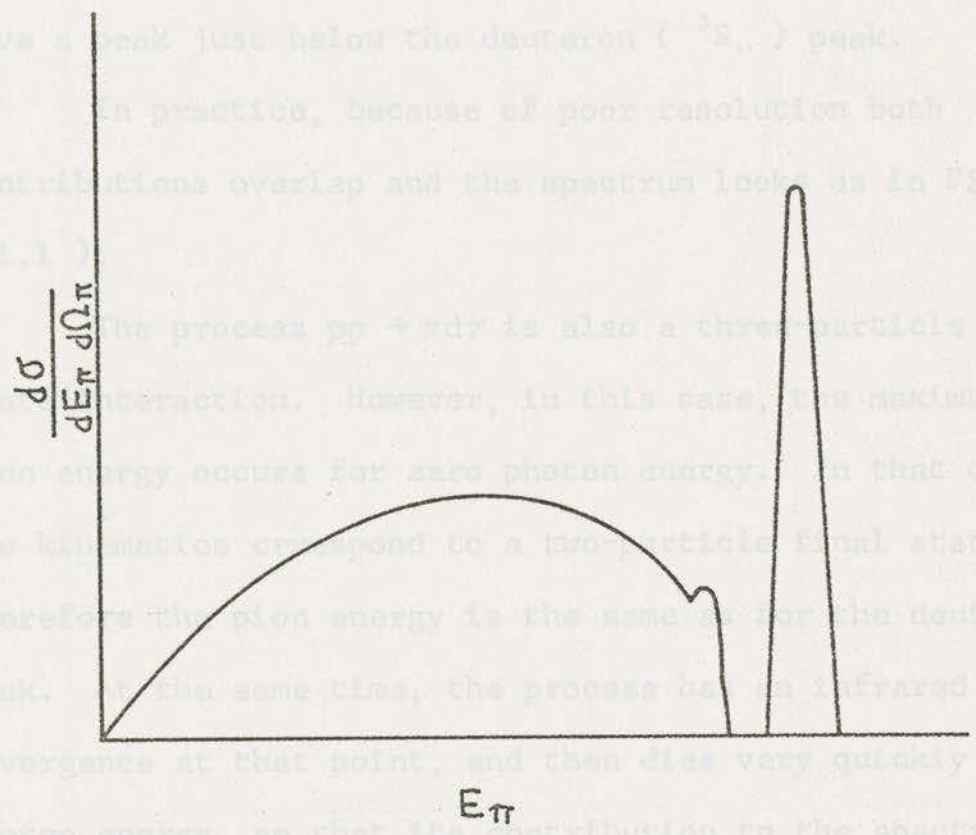


Figure 3.2 Pion spectrum for two- and three- particle final states with high resolution showing the possible 1S_0 peak

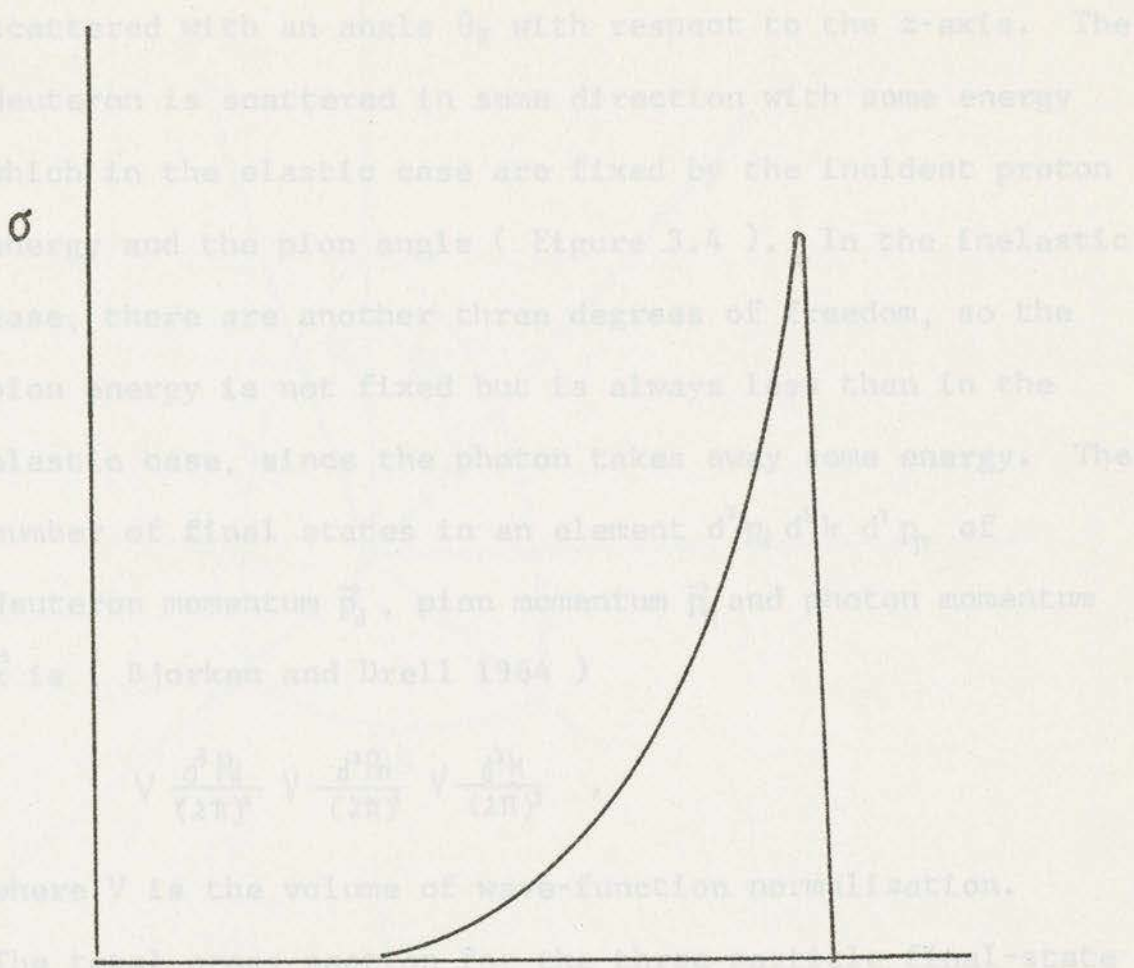
The kinematics can be described as follows. The proton is incident along the z-axis and the target proton is at rest at the origin of coordinates. The pion is

process. The latter is dominated by the 3S_1 and 1S_0 states of the p-n system. The 1S_0 state is believed to have a peak just below the deuteron (3S_1) peak.

In practice, because of poor resolution both contributions overlap and the spectrum looks as in Figure (1.1).

The process $pp \rightarrow \pi d \gamma$ is also a three-particle final state interaction. However, in this case, the maximum pion energy occurs for zero photon energy. In that case, the kinematics correspond to a two-particle final state and therefore the pion energy is the same as for the deuteron peak. At the same time, the process has an infrared divergence at that point, and then dies very quickly with photon energy, so that its contribution to the spectrum is as shown in Figure (3.3). An evaluation of the cross section for $pp \rightarrow \pi d \gamma$ will thus tell us whether or not this process should be taken into account when looking at $pp \rightarrow \pi pn$ with high resolution near the upper end of the spectrum.

Figure 3.3 Expected radiative tail from the process $pp \rightarrow \pi d \gamma$. The kinematics can be described as follows. The proton is incident along the z-axis and the target proton is at rest at the origin of coordinates. The pion is



reaction $pp \rightarrow \pi d$ is E_{π} .

$$\sigma = \int V \frac{d^3 p_1}{(2\pi)^3} \frac{d^3 p_2}{(2\pi)^3} \frac{d^3 k}{(2\pi)^3} \frac{1}{J_{inc} V} w_{fi} \quad (3.1)$$

where J_{inc} is the incident proton flux, V is the number of particles per unit volume, and w_{fi} is the transition rate

Figure 3.3 Expected radiative tail from the process $pp \rightarrow \pi d$

In natural units ($\hbar = c = 1$), w_{fi} is written as

scattered with an angle θ_π with respect to the z-axis. The deuteron is scattered in some direction with some energy which in the elastic case are fixed by the incident proton energy and the pion angle (Figure 3.4). In the inelastic case, there are another three degrees of freedom, so the pion energy is not fixed but is always less than in the elastic case, since the photon takes away some energy. The number of final states in an element $d^3 p_d d^3 k d^3 p_\pi$ of deuteron momentum \vec{p}_d , pion momentum \vec{p}_π and photon momentum \vec{k} is (Bjorken and Drell 1964)

$$V \frac{d^3 p_d}{(2\pi)^3} V \frac{d^3 p_\pi}{(2\pi)^3} V \frac{d^3 k}{(2\pi)^3} ,$$

where V is the volume of wave-function normalization.

The total cross section for the three particle final-state reaction $pp \rightarrow \pi d \gamma$ is then,

$$\sigma = \int V^3 \frac{d^3 p_d}{(2\pi)^3} \frac{d^3 p_\pi}{(2\pi)^3} \frac{d^3 k}{(2\pi)^3} \frac{1}{J_{\text{incl}} \frac{1}{V}} w_{fi} , \quad (3.1)$$

where J_{inc} is the incident proton flux, $\frac{1}{V}$ is the number of particles per unit volume, and w_{fi} is the transition rate from the incident state to the final state.

In natural units ($c = \hbar = 1$), w_{fi} is written as

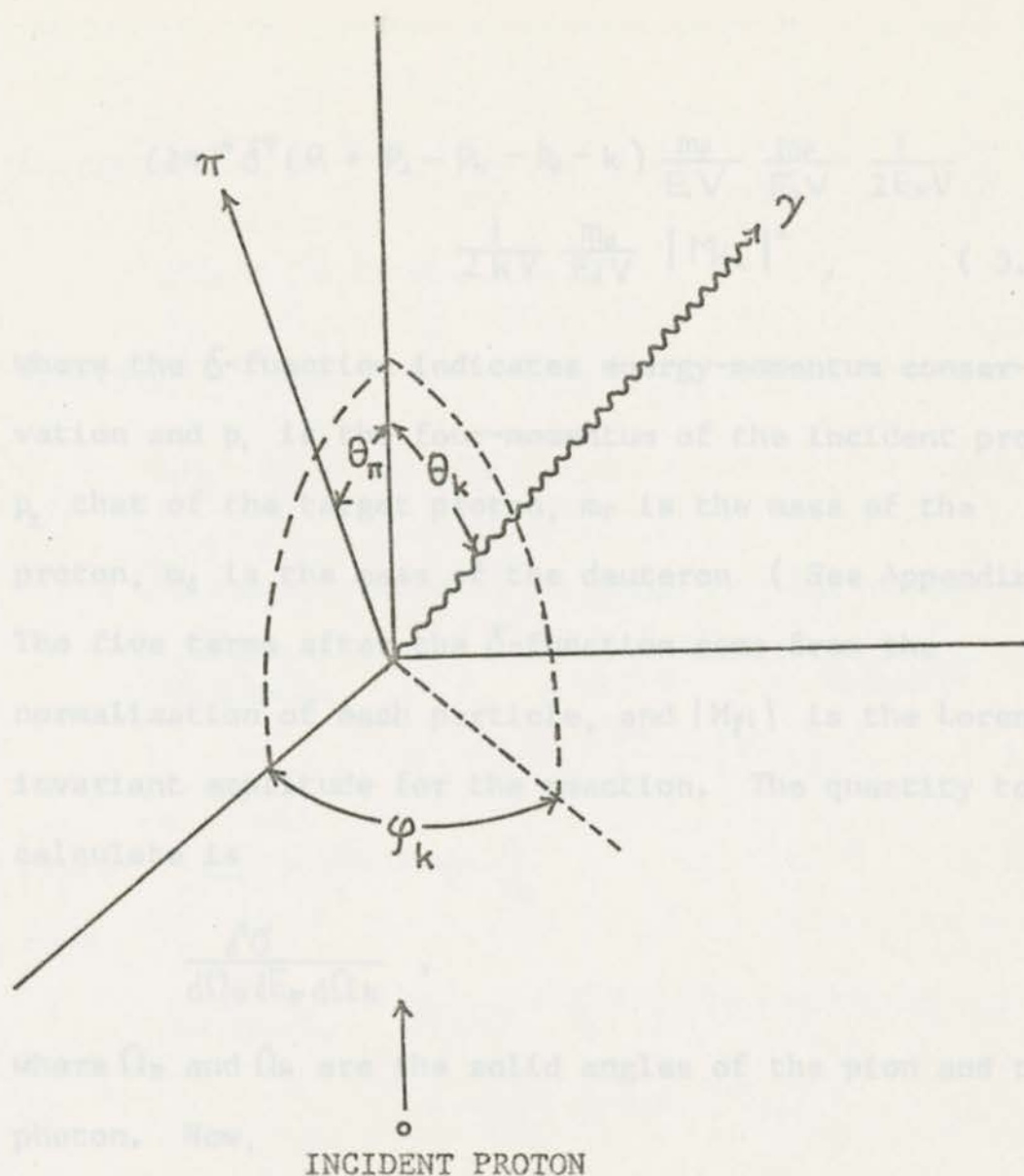


Figure 3.4 Three-dimensional Laboratory kinematics

$$(2\pi)^4 \delta^4(p_1 + p_2 - p_\pi - p_d - k) \frac{m_p}{E_1 V} \frac{m_p}{E_2 V} \frac{1}{2E_\pi V} \\ \frac{1}{2kV} \frac{m_d}{E_d V} |M_{fi}|^2, \quad (3.2)$$

where the δ -function indicates energy-momentum conservation and p_1 is the four-momentum of the incident proton, p_2 that of the target proton, m_p is the mass of the proton, m_d is the mass of the deuteron (See Appendix A). The five terms after the δ -function come from the normalization of each particle, and $|M_{fi}|$ is the Lorentz invariant amplitude for the reaction. The quantity to calculate is

$$\frac{d^3\sigma}{d\Omega_\pi dE_\pi d\Omega_k},$$

where Ω_π and Ω_k are the solid angles of the pion and the photon. Now,

$$d^3p_\pi = p_\pi^2 dp_\pi d\Omega_\pi. \quad (3.3)$$

But p_π satisfies

$$p_\pi^2 = E_\pi^2 - m_\pi^2; \quad (3.4)$$

then

$$p_\pi dp_\pi = E_\pi dE_\pi, \quad (3.5)$$

therefore

$$d^3P_\pi = P_\pi E_\pi dE_\pi d\Omega_\pi. \quad (3.6)$$

Similarly

$$d^3k = k^2 dk d\Omega_k. \quad (3.7)$$

Since the target proton is at rest, $E_2 = m_p$, therefore

$$\begin{aligned} \frac{d^3\sigma}{d\Omega_\pi dE_\pi d\Omega_k} &= \int \frac{\delta^4(P_1 + P_2 - P_\pi - P_d - k)}{(2\pi)^5 4} \frac{m_p m_d d^3P_d}{E_p E_\pi k E_d} \\ &\times \frac{P_\pi E_\pi k^2 dk}{V |J_{inc}|} |M_{fi}|^2, \end{aligned} \quad (3.8)$$

$$\text{where } J_{inc} = \frac{V_p}{V} = \frac{1}{V} \frac{P_p}{E_p}. \quad (3.9)$$

Thus

$$\begin{aligned} \frac{d^3\sigma}{d\Omega_\pi dE_\pi d\Omega_k} &= \frac{1}{2(2\pi)^5} \frac{m_p m_d}{P_p} \int \delta^4(P_1 + P_2 - P_\pi - P_d - k) \\ &\times \frac{d^3P_d}{2E_d} P_\pi k dk |M_{fi}|^2. \end{aligned} \quad (3.10)$$

Note that

$$\frac{d^3P_d}{2E_d} = \int d^4P_d \delta(P_d^2 - m_d^2) \theta(E_d), \quad (3.11)$$

so that

$$\begin{aligned} \frac{d^3\sigma}{d\Omega_\pi dE_\pi d\Omega_k} &= \frac{m_p m_d}{2(2\pi)^5 P_p} \int \delta^4(P_1 + P_2 - P_\pi - P_d - k) \\ &\times \delta(P_d^2 - m_d^2) d^4P_d P_\pi k dk |M_{fi}|^2 \\ &= \frac{m_p m_d}{2(2\pi)^5 P_p} \int \delta(P_d^2 - m_d^2) P_\pi k |M_{fi}|^2 dk \end{aligned} \quad (3.12)$$

$$= \frac{1}{2(2\pi)^5} \frac{m_p m_d}{P_p} \frac{P_\pi k |M_{fi}|^2}{\frac{\partial(P_d^2 - m_d^2)}{\partial k}}, \quad (3.13)$$

where the relation

$$\int g(p) \delta(f(p)) dP = \frac{g(f(p)=0)}{\left. \frac{\partial f(p)}{\partial P} \right|_{f(p)=0}} \quad (3.14)$$

has been used. Now

$$\begin{aligned} \frac{\partial(P_d^2 - m_d^2)}{\partial k} &= \frac{\partial}{\partial k} \{ -2k(P_1 + P_2 - P_\pi) \} \\ &= \{ \vec{n} \cdot (\vec{P}_p - \vec{P}_\pi) - (E_p + m_p - E_\pi) \}, \end{aligned} \quad (3.15)$$

where \vec{n} is $\frac{\vec{k}}{k}$. Then

$$\frac{d^3\sigma}{d\Omega_\pi dE_\pi d\Omega_k} = \frac{1}{4(2\pi)^5} \frac{m_p m_d P_\pi k |M_{fi}|^2}{P_p \{ \vec{n} \cdot (\vec{P}_p - \vec{P}_\pi) - (E_p + m_p - E_\pi) \}}. \quad (3.16)$$

The photon energy must be calculated and expressed in terms of the photon angles, so that the integration over all photon angles can be carried out. The equation for the energy-momentum conservation of this system is

$$P_1 + P_2 = P_\pi + P_d + k \quad (3.17)$$

and obtain

$$\text{or } (P_1 + P_2 - P_\pi - k)^2 = P_d^2. \quad (3.18)$$

Expand this to

$$-2k(P_1 + P_2 - P_\pi) + (P_1 + P_2 - P_\pi)^2 = m_d^2 \quad (3.19)$$

Rearranging terms, the expression becomes

$$\text{or } 2k(E_p + m_p - E_\pi) - 2\vec{k} \cdot (\vec{P}_p - \vec{P}_\pi) = \quad (3.20)$$

$$(P_1 + P_2 - P_\pi)^2 - m_d^2 \quad (3.20)$$

$$\text{Then } k = \frac{m_p^2 + m_\pi^2 + m_\pi^2 - 2P_1 P_\pi - 2P_2 P_\pi + 2P_1 P_2 - m_d^2}{2 \{ (E_p + m_p - E_\pi) - \vec{n} \cdot (\vec{P}_p - \vec{P}_\pi) \}} ,$$

and finally

$$k = \frac{2m_p^2 + m_\pi^2 - m_d^2 - 2E_p E_\pi + 2\vec{P}_p \cdot \vec{P}_\pi - 2m_p E_\pi + 2E_p m_p}{2 \{ (E_p + m_p - E_\pi) - \vec{n} \cdot (\vec{P}_p - \vec{P}_\pi) \}} \quad (3.21)$$

For the elastic case $pp \rightarrow \pi d$, the cross section is similarly given by

$$\sigma^{el} = \int V^2 \frac{d^3 P_d}{(2\pi)^3} \frac{d^3 P_\pi}{(2\pi)^3} \frac{m_d}{E_d V} \frac{1}{2E_\pi V} \frac{m_p}{E_1 V} \frac{m_p}{E_2 V} \frac{1}{\frac{1}{V} |J_{inc}|} \\ \times (2\pi)^4 \delta^4(P_1 + P_2 - P_\pi - P_d) |M_{fi}^d|^2 \quad (3.22)$$

As done earlier, one can make the replacement

$$E_2 \rightarrow m_p, \quad E_1 \rightarrow E_p$$

$$V |J_{inc}| \rightarrow \frac{P_p}{E_p}$$

$$d^3 P_\pi \rightarrow P_\pi E_\pi dE_\pi d\Omega_\pi$$

and obtain

$$\frac{d\sigma^{el}}{d\Omega_\pi} = \frac{1}{2(2\pi)^2} \int d^3 P_d P_\pi E_\pi dE_\pi \frac{m_d}{E_d} \frac{1}{E_\pi} \frac{m_p}{E_p} \frac{E_p}{P_p} \\ \times \delta^4(P_1 + P_2 - P_\pi - P_d) |M_{fi}^{el}|^2 \quad (3.23)$$

Rearranging terms, the expression becomes

$$\frac{1}{(2\pi)^2} \frac{m_d m_p}{P_p} \int \frac{d^3 P_d}{2E_d} P_\pi dE_\pi \delta^4(P_1 + P_2 - P_\pi - P_d) |M_{fi}^{el}|^2 \quad (3.24)$$

Using the same method for p_d , the expression becomes

$$\frac{1}{(2\pi)^2} \frac{m_d m_p}{p_p} \int d^3 p_d \delta(p_d^2 - m_d^2) \delta^4(p_1 + p_2 - p_\pi - p_d) \times |M_{fi}^{el}|^2 p_\pi dE_\pi, \quad (3.25)$$

and calculating the integral in p_d , it becomes

$$\frac{1}{(2\pi)^2} \frac{m_d m_p}{p_p} \int \delta(p_d^2 - m_d^2) p_\pi |M_{fi}^{el}|^2 dE_\pi, \quad (3.26)$$

and finally

$$\frac{1}{(2\pi)^2} \frac{m_d m_p}{p_p} \frac{p_\pi |M_{fi}^{el}|^2}{\frac{\partial(p_d^2 - m_d^2)}{\partial E_\pi}}. \quad (3.27)$$

Now

$$\begin{aligned} \frac{\partial p_d^2}{\partial E_\pi} &= \frac{\partial}{\partial E_\pi} \{-2p_\pi (p_1 + p_2)\} \\ &= \frac{\partial}{\partial E_\pi} \{-2E_\pi (E_p + m_p) + 2\vec{p}_\pi \cdot \vec{p}_p\}, \end{aligned} \quad (3.28)$$

and

$$\frac{\partial \vec{p}_\pi}{\partial E_\pi} = \vec{p}_\pi \frac{E_\pi}{p_\pi^2}, \quad (3.29)$$

so that

$$\frac{\partial p_d^2}{\partial E_\pi} = -2(E_p + m_p) + 2 \frac{\vec{p}_\pi \cdot \vec{p}_p}{p_\pi^2} E_\pi. \quad (3.30)$$

Thus,

$$\frac{d\sigma^{el}}{d\Omega_\pi} = \frac{1}{(2\pi)^2} \frac{m_p m_d}{2p_p} \frac{p_\pi^3 |M_{fi}^{el}|^2}{\vec{p}_\pi \cdot \vec{p}_p E_\pi - p_\pi^2 (E_p + m_p)}. \quad (3.31)$$

The kinematics for both the elastic ($pp \rightarrow \pi d$) and inelastic ($pp \rightarrow \pi d\gamma$) reactions have now been dealt with fully. It remains to deal with the dynamical problem of evaluating M_{fi} . The evaluation depends on the particular approach used. As mentioned earlier, a soft-photon calculation is relatively simple and quite appropriate for this problem, since we are interested in low-energy photon emission. This approach will be described in the following chapters.

CHAPTER 4GENERAL FEYNMAN RULES FOR A CHARGED PARTICLE

The perturbative approach taken by Feynman in calculating scattering amplitudes can be described basically as follows: the state after scattering is obtained by operating on the state before scattering with a propagator operator. If the incident particle is normalized, the transition amplitude to the state one measures is defined as the projection of the scattered state to the measured state. It is difficult to determine the exact propagator, but it can be expressed as an expansion in terms of the propagator for a free particle. The propagator for a free particle turns out to be a time-dependent Green's function. High-order terms of the expansion contain a greater number of interactions between the particles. The n -th term contains n interactions. High-order terms can be neglected since the "coupling", or interaction strength, is small and the expansion converges quickly. Propagator for protons and for pions are derived in the following way.

The proton wave function must satisfy the Dirac

equation. The Dirac equation for free particles is

$$i\hbar \left(\gamma^0 \frac{\partial}{\partial x^0} + \gamma^1 \frac{\partial}{\partial x^1} + \gamma^2 \frac{\partial}{\partial x^2} + \gamma^3 \frac{\partial}{\partial x^3} \right) \psi - mc\psi = 0, \quad (4.1)$$

where the γ^μ ($\mu = 0, 1, 2, 3$) are called gamma matrices, and satisfy the following commutation relation.

$$\gamma^\mu \gamma^\nu + \gamma^\nu \gamma^\mu = 2g^{\mu\nu}. \quad (4.2)$$

The explicit representation for the gamma matrices which is commonly used is presented in the Appendix. In operator notation, the equation is written as

$$(\gamma^\mu p_\mu - m)\psi = 0, \quad (4.3)$$

in natural units ($c = \hbar = 1$). $\gamma^\mu B_\mu$, where B_μ is any 4-vector, is commonly written as \not{B} .

To describe an electromagnetic interaction, the coupling is introduced simply by replacing p_μ by $p_\mu - \frac{e}{c}A_\mu$, where $A_\mu = (\phi, -\vec{A})$ are the scalar and vector potentials respectively (Schiff 1968). Thus the Dirac equation becomes

$$\{(\not{p} - eA) - m\}\psi = 0. \quad (4.4)$$

One can rearrange this to

$$(\not{\partial} - m)\psi = eA\psi. \quad (4.5)$$

$\psi(x,t)$ can be expressed as

$$\psi(x) = \phi_L(x) + \int G(x,x') eA(x') \psi(x') d^4x', \quad (4.6)$$

where $G(x,x')$ is the Green's function and $\phi_L(x)$ is the wave function which satisfies the free Dirac equation. Because $\phi_L(x)$ is a free wave, it can be interpreted as the incident wave in the remote past. As mentioned before, G is the free propagator. Then, G is written in terms of free waves at points x and y as

$$G(x,y) = -i \sum_r \phi_r(x) \bar{\phi}_r(y),$$

where r is summed over the complete set of functions at points x and y , and $\bar{\phi}$ is defined as $\phi^\dagger \gamma_0$. The Dirac equation also has negative-energy solutions. But no negative-energy particles are involved in our calculations; thus, the negative energy waves are subtracted from the above Green function, and r now covers all positive-energy functions (Schweber 1955). Thus, Equation (4.6) is now

$$\psi(x) - \phi_L(x) = -ie \sum_r \phi_r(x) \int d^4y \bar{\phi}_r(y) A(y) \psi(y). \quad (4.6)$$

Therefore, the S-matrix for a transition between initial state i and final state f is

$$S_{fi} = \delta_{fi} - ie \int \bar{\Phi}_f A \psi d^4y. \quad (4.7)$$

Using $\psi(x)$ given in Equation (4.6) and iterating, one obtains

$$S_{fi} = \delta_{fi} - ie \int d^4x \bar{\Phi}_f A \Phi_i - ie^2 \int d^4x_2 d^4x_1 \bar{\Phi}_f G(x_2, x_1) A(x_1) \Phi_i(x_1) \\ - \dots - ie^n \int d^4x_n \dots d^4x_1 \bar{\Phi}_f(x_n) A(x_n) G(x_n, x_{n-1}) \dots G(x_2, x_1) A(x_1) \Phi_i(x_1) - \dots$$

The third term is interpreted as follows; the incident wave is modified by the first interaction $A(x_1)$ which takes place at a certain time t_1 (zeroth component of x_1) during the interval considered. The state that follows the interaction can be obtained by adding all contributions from the points on the trajectories in space-time. $G(x_2, x_1)$ propagates the modified wave from the point x_1 to the point x_2 . The modified wave interacts again with $A(x_2)$ at point x_2 and becomes a new state.

To derive $G(x, x')$ explicitly, one uses one of the characteristics of the Green's function. The Green's function will satisfy

$$(\not{\partial} - m) G(x, x') = \delta^4(x - x'). \quad (4.8)$$

$G(x, x')$ can be expressed as a Fourier integral

$$G(x, x') = \frac{1}{(2\pi)^4} \int G(p) \exp[-ip(x-x')] d^4p. \quad (4.9)$$

$$\text{Similarly, } \delta^4(x-x') = \frac{1}{(2\pi)^4} \int \exp[-ip(x-x')] d^4p. \quad (4.10)$$

Substituting these two equations into Equation (4.8),

one obtains (Bjorken and Drell 1964)

$$G(p) = \frac{1}{\not{p} - m} = \frac{\not{p} + m}{p^2 - m^2 + i\varepsilon} \quad (4.11)$$

where $\varepsilon \rightarrow 0^+$ insures that the positive energy wave propagates to the future and the negative wave to the past.

Note that the interaction with the electromagnetic field is expressed as $e\hat{A}$ in the integral equation. For the case of a free photon of momentum \vec{k} , the electromagnetic field is expressed as

$$A^\mu(x) = \frac{\epsilon^\mu}{\sqrt{2kV}} \{ \exp(-ikx) + \exp(ikx) \} \quad (4.12)$$

where ϵ^μ is the unit polarization vector. The first term for which the energy δ function is $\delta(E_i + k - E_f)$ describes absorption of energy in the scattering process and does not contribute to the process of interest. Thus, the interaction of the proton with the photon in momentum space is expressed as $e\hat{p}$, apart from normalization constants.

The combined expression for an incident proton which emits a photon is

$$\frac{\not{p} + m_p}{p^2 - m_p^2} e \not{\epsilon} | p_p \rangle, \quad (4.13)$$

in momentum space, where $p = p_p - k$. Since $p^2 = (p_p - k)^2 = m_p^2 - 2p_p \cdot k \neq m_p^2$, the proton is off the mass shell after photon emission. This process is shown in the Figure (4.1a).

In the case of a pion, the wave function must satisfy the Klein-Gordon equation

$$\{ \square + \left(\frac{mc}{\hbar} \right)^2 \} \psi = 0, \quad (4.14)$$

where $\square \equiv \frac{\partial^2}{\partial x_\mu \partial x^\mu}$.

In terms of momentum operators, the equation is written as

$$(-p_\mu p^\mu + m^2) \psi = 0, \quad (4.15)$$

in natural units. Where there is an electromagnetic interaction, again replace p_μ by $p_\mu - eA_\mu$, and obtain

$$\{ -(p_\mu - eA_\mu)(p^\mu - eA^\mu) + m^2 \} \psi = 0, \quad (4.16)$$

or

$$(-p_\mu p^\mu + m^2) \psi = \{ -e(p_\mu A^\mu + A_\mu p^\mu) + eA_\mu A^\mu \} \psi. \quad (4.17)$$

By using the Green's function $\Delta_F(x, x_1)$, one obtains

$$\Psi(x, t) = \varphi(x, t) + \int d^4x_1 \Delta_F(x, x_1) V(x_1) \Psi(x_1), \quad (4.18)$$

where $V(x_1) = e(p_\mu A^\mu + A_\mu p^\mu) - e^2 A_\mu A^\mu$ (4.19)

and $\varphi(x, t)$ is a free pion wave function. $\Delta_F(x, x_1)$ is derived as before by using

$$(-p^2 + m^2) \Delta_F(x, x_1) = -\delta^4(x - x_1). \quad (4.20)$$

$\Delta_F(x, x_1)$ is expressed as

$$\Delta_F(x, x_1) = \int \frac{d^4p}{(2\pi)^4} \Delta_F(p) \exp[-ip(x - x_1)]. \quad (4.21)$$

$\delta^4(x - x_1)$ is also written as

$$\delta^4(x - x_1) = \int \frac{d^4p}{(2\pi)^4} \exp[-ip(x - x_1)]. \quad (4.22)$$

Then, $\Delta_F(p) = \frac{1}{p^2 - m^2 + i\epsilon}$. (4.23)

The S-matrix is defined as

$$S_{fi} = \delta_{fi} - i \int d^4y \Phi_f^* V \psi. \quad (4.27)$$

Using $\Psi(x)$ given in Equation (4.18) and iterating, one obtains

$$\begin{aligned} S_{fi} = & \delta_{fi} - i \int d^4x \Phi_f^* V \varphi - i \int d^4x_2 d^4x_1 \Phi_f^* V \Delta_F(x, x_1) V(x_1) \varphi(x_1) \\ & - \dots - i \int d^4x_n \dots d^4x_1 \Phi_f^*(x_n) V(x_n) \Delta(x_n, x_{n-1}) \dots \varphi(x_1). \end{aligned} \quad (4.24)$$

Now in the integral of Equation (4.24), the term

$$\Delta_F(x, x_1) e (p_\mu A^\mu + A_\mu p^\mu) , \quad (4.25)$$

where the lowest order in V is taken, is interpreted as follows: the free spin-zero particle, which may be off the mass shell, operated from the right interacts with the electromagnetic field, is modified by the field and propagated to the point x . Therefore, if one writes the particles after and before the interaction with the field as $|f\rangle$ and $|i\rangle$ respectively, the matrix element of this process is

$$\langle f | p_\mu A^\mu + A_\mu p^\mu | i \rangle . \quad (4.26)$$

The first p_μ operates on the $\langle f |$ state or the state after the interaction and the second p^μ operates on the $|i\rangle$ state or the state before the interaction. Then,

$$\langle f | p_{f\mu} A^\mu + A_\mu p_i^\mu | i \rangle = \langle f | (p_f + p_i)_\mu A^\mu | i \rangle , \quad (4.27)$$

where p_f is the momentum of $\langle f |$ state and p_i is the momentum of $|i\rangle$ state. Then, the interaction between a pion and a photon is expressed as

$$e (p_i + p_f)_\mu \epsilon^\mu \quad (4.28)$$

in momentum space, where ϵ^μ is the polarization of the

photon. Therefore, the process in which the pion, modified in the strong interaction, propagates to the point where it emits a photon and becomes a pion in a certain state is expressed as

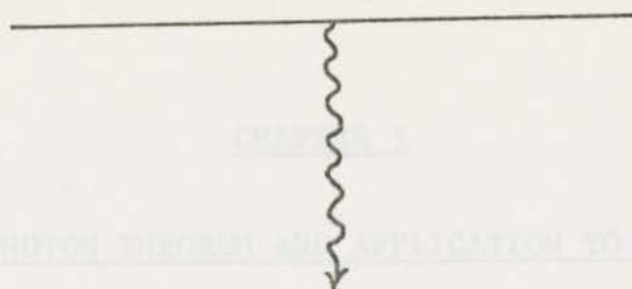
$$\langle P_\pi | e (P_f + P_i)_\mu \epsilon^\mu \frac{1}{P_i^2 - m_\pi^2 + i\epsilon} \quad (4.29)$$

in momentum space. From energy-momentum conservation,

$$P_f = P_\pi \quad P_i = P_\pi + k .$$

Since the square of the four-momentum of the pion before the electromagnetic interaction is not m_π^2 , the pion before photon emission is not on the mass shell. This process is shown in Figure (4.1b).

Figure 4.1b Photon-pion vertex



CHAPTER 4
SOFT-PHOTON THEOREM AND APPLICATION TO SPINLESS
CHARGED-PARTICLE SCATTERING

Figure 4.1a Photon-nucleon vertex

For the pion, the process of photon emission is

described by

$$(R_+ | e(2R_+ + k) \gamma^5 | R_+ + k \rangle \frac{1}{(R_+ + k)^2 - m_\pi^2} \quad (3.1)$$

The denominator of the propagator obeys

$$(R_+ + k)^2 - m_\pi^2 = 2R_+ k$$

Thus, one obtains

$$(R_+ | e(2R_+ + k) \gamma^5 | R_+ + k \rangle \frac{1}{2R_+ k}$$

or

Figure 4.1b Photon-pion vertex

$$\frac{e(2R_+ + k) \gamma^5}{2R_+ k} | R_+ + k \rangle \quad (3.2)$$

Gauge invariance requires that $k_\mu \epsilon^\mu = 0$, therefore we left

with

CHAPTER 5

SOFT-PHOTON THEOREM AND APPLICATION TO SPINLESS
CHARGED-PARTICLE SCATTERING

Using the Feynman rules derived in the preceding chapter, one can easily show that photon emission by the external particle has infrared divergences.

For the pion, the process of photon emission is described by

$$\langle P_\pi | e(2P_\pi + k)_\mu \epsilon^\mu \frac{1}{(P_\pi + k)^2 - m_\pi^2} \rangle. \quad (5.1)$$

The denominator of the propagator obeys

$$(P_\pi + k)^2 - m_\pi^2 = 2P_\pi k.$$

Thus, one obtains

$$\langle P_\pi | e(2P_\pi + k)_\mu \epsilon^\mu \frac{1}{2P_\pi k},$$

or

$$\frac{e(2P_\pi + k)_\mu \epsilon^\mu}{2P_\pi k} \langle P_\pi + k |. \quad (5.2)$$

Gauge invariance requires that $k_\mu \epsilon^\mu = 0$, then one is left with

$$\frac{e P_{\pi} \epsilon^{\mu}}{P_{\pi} k} \langle P_{\pi} + k | \quad . \quad (5.3)$$

Clearly this expression diverges as $k \rightarrow 0$ (infrared limit).

For the proton the process of photon emission is described by

$$\frac{P_p - k + m_p}{(P_p - k)^2 - m_p^2} \not{\epsilon} | P_p \rangle \quad . \quad (5.4)$$

The denominators and the numerator become

$$\frac{-\not{\epsilon} (P_p - k - m_p) + 2\epsilon P_p - 2k\epsilon}{-2P_p k} | P_p \rangle \quad .$$

This also diverges as k goes to zero.

Now the external proton obeys the Dirac equation

$$(P_p - m_p) | P_p \rangle = 0 \quad . \quad (5.5)$$

So the amplitude behaves as

$$\frac{\not{\epsilon} k + 2\epsilon P_p}{-2P_p k} | P_p \rangle \quad . \quad (5.6)$$

Now, when k is very small this becomes

$$-\frac{\epsilon P_p}{P_p k} | P_p \rangle \quad . \quad (5.7)$$

Thus, when the photon energy is small, we may consider the

proton as a spinless particle. We should note that the infrared divergent emissions take place only at the two cases mentioned above.

An internal particle off the mass shell doesn't create a divergence, since the denominator of the particle will be

$$(P \pm k)^2 - m^2 = p^2 - m^2 \pm 2Pk, \quad (5.8)$$

where $p^2 \neq m^2$.

Also a direct channel resonance in the interaction does not create a divergence, since the propagator includes a width, i.e.

$$\frac{1}{(P \pm k)^2 - m^2 + i\Gamma} = \frac{1}{p^2 - m^2 \pm 2Pk + i\Gamma} = \frac{1}{\pm 2Pk + i\Gamma}, \quad (5.9)$$

where Γ is the width.

The presence of Γ prevents a divergence as $k \rightarrow 0$.

Let the bremsstrahlung amplitude for any spinless-particle scattering process be written as $\epsilon_\mu M_\mu$ and specifically, $\epsilon^\mu M_\mu^{(1)}$ for the photon emission from the processes of external particle emission. (Figure 5.1a)

Then

$$M_{\mu} = M_{\mu}^{(1)} + M_{\mu}^{(2)} \quad (5.10)$$

where $M_{\mu}^{(1)}$ is the amplitude which includes all process of internal emission (Figure 5.1b).

For simplicity, assume that only one particle is charged. Let $T(\nu, \Delta)$ be the strong amplitude, which depends on the usual two variables.

$$\nu = p_1 p_2 + p_3 p_4 \quad \Delta = p_1 p_3 + p_2 p_4 \quad (5.11)$$

and let $T_1(k, \nu, \Delta)$ and $T_2(k, \nu, \Delta)$ be the amplitude for radiation by the incoming and outgoing charged particle respectively.

Then, when the photon is not emitted, the amplitude must be equal to the strong amplitude,

$$T(\nu, \Delta) = T_1(0, \nu, \Delta) = T_2(0, \nu, \Delta) . \quad (5.12)$$

Using the results of the previous chapter, one writes $M_{\mu}^{(1)}$ as

$$\frac{e p_{2\mu}}{p_2 k} T_2 - \frac{e p_{1\mu}}{p_1 k} T_1 . \quad (5.13)$$

Expand T_1 , T_2 in terms of k around $k = 0$

$$M_{\mu}^{(1)} = \left(\frac{e p_{2\mu}}{p_2 k} - \frac{e p_{1\mu}}{p_1 k} \right) T + \frac{e p_{2\mu}}{p_2 k} \left(\frac{\partial T_2}{\partial k_{\mu}} \Big|_{k=0} k_{\mu} \right)$$

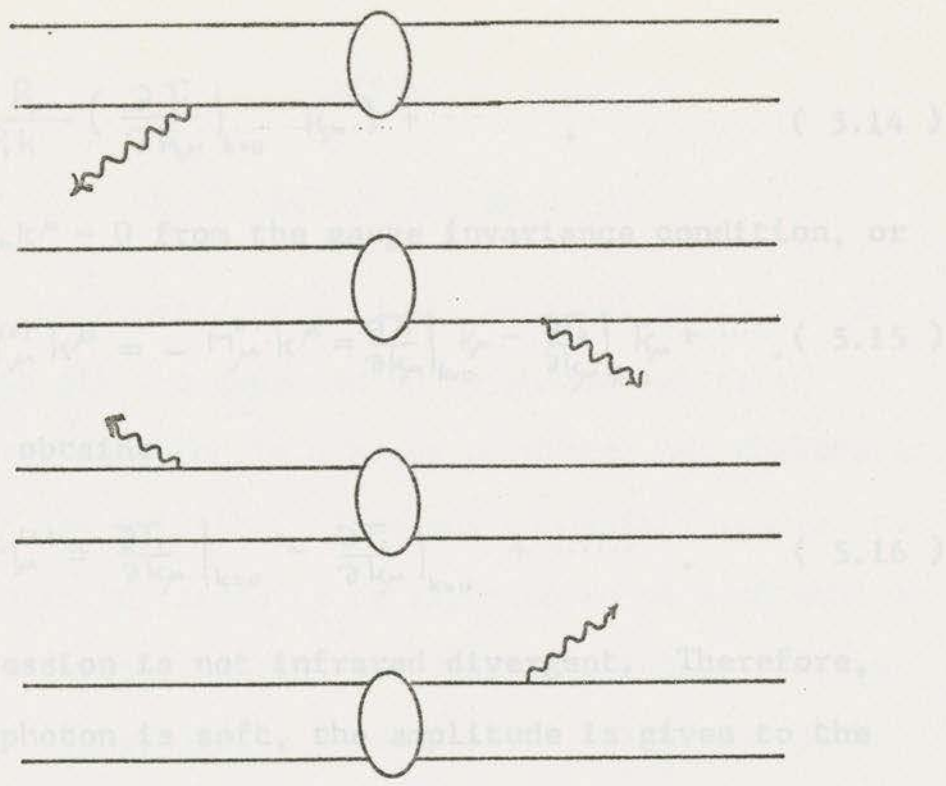


Figure 5.1a Photon emission from external particles

$$M_{\mu} = e \left(\frac{\partial}{\partial k^{\mu}} - \frac{\partial}{\partial k^{\nu}} \right) T \quad (5.17)$$

where T is now the strong amplitude on the mass shell.

(Piccolotto 1972).

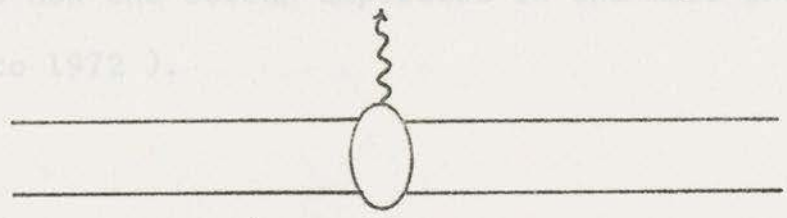


Figure 5.1b Photon emission from internal particles

$$- \frac{e P_{\mu}}{P_1 k} \left(\frac{\partial T_1}{\partial k_{\mu}} \Big|_{k=0} k_{\mu} \right) + \dots \quad (5.14)$$

But now $M_{\mu} k^{\mu} = 0$ from the gauge invariance condition, or

$$M_{\mu}^{(2)} k^{\mu} = - M_{\mu}^{(1)} k^{\mu} = \frac{\partial T_1}{\partial k_{\mu}} \Big|_{k=0} k_{\mu} - \frac{\partial T_2}{\partial k_{\mu}} \Big|_{k=0} k_{\mu} + \dots \quad (5.15)$$

Then, one obtains

$$M_{\mu}^{(2)} = \frac{\partial T_1}{\partial k_{\mu}} \Big|_{k=0} - \frac{\partial T_2}{\partial k_{\mu}} \Big|_{k=0} + \dots \quad (5.16)$$

This expression is not infrared divergent. Therefore, when the photon is soft, the amplitude is given to the lowest order in k by

$$M_{\mu} = e \left(\frac{P_{2\mu}}{P_2 k} - \frac{P_{1\mu}}{P_1 k} \right) T \quad (5.17)$$

where T is now the strong amplitude on the mass shell.

(Picciotto 1972).

$$M_{\mu} \epsilon^{\mu} = e \left(\frac{p_{2\mu} \epsilon^{\mu}}{P_2 k} - \frac{p_{1\mu} \epsilon^{\mu}}{P_1 k} \right) T \quad (6.1)$$

where p_1 has been replaced by p_2 and p_2 by p_1 in the result of the previous chapter. As required, this satisfies the gauge invariance condition.

$$M_{\mu} k^{\mu} = 0 \quad (6.2)$$

CHAPTER 6

CROSS SECTION FOR $pp \rightarrow \pi d \gamma$

In the process $pp \rightarrow \pi d$ all external particles are charged and all are expected to be photon emitters.

However, the deuteron is a heavy particle, and therefore emerges at low velocity. Thus one can safely ignore its photon radiation, since it is expected to be much smaller than the contribution from the other particles. In the laboratory frame, photon emission from the target proton can also be ignored; this can easily be seen in the transverse gauge $\epsilon = (0, \vec{\epsilon})$, in which case $p\epsilon = 0$.

Thus, one only needs to consider emission by the incoming proton and outgoing pion. In this case, the amplitude in the lowest order is

$$M_\mu \epsilon^\mu = e \left(\frac{p_{\pi\mu} \epsilon^\mu}{p_\pi \cdot k} - \frac{p_{p\mu} \epsilon^\mu}{p_p \cdot k} \right) T \quad (6.1)$$

where p_1 has been replaced by p_p and p_2 by p_π in the result of the previous chapter. As required, this satisfies the gauge invariance condition.

$$M_\mu k^\mu = 0 \quad (6.2)$$

Now one must add $|M_{\mu} \epsilon^{\mu}|^2$ over photon polarizations, since the photon polarization is not measured. To do so by employing Feynman's technique, one orients the coordinates such that

$$k = (k^0, k', 0, 0), \quad (6.3)$$

where

$$k^0 = k' = k. \quad (6.4)$$

Suppose there are two currents a^{μ} and b^{μ} satisfying the gauge condition.

$$k_{\mu} a^{\mu} = k_{\mu} b^{\mu} = 0. \quad (6.5)$$

One needs to evaluate

$$\sum_{\text{pol}} \epsilon_{\mu} a^{\mu} \epsilon_{\nu} b^{\nu}. \quad (6.6)$$

Since this is a scalar, one can choose the frame in which the zeroth component of the polarization vanishes. Then the photons are transverse, and ϵ can have two possible directions

$$\epsilon_1^{\mu} = (0, 0, 1, 0) \quad \epsilon_2^{\mu} = (0, 0, 0, 1). \quad (6.7)$$

Then equation (6.1). If one takes the average over the

$$\sum_{\text{pol}} \epsilon_{\mu} a^{\mu} \epsilon_{\nu} b^{\nu} = a^{\mu} b^{\mu} = a^0 b^0 - a^1 b^1 - a^2 b^2. \quad (6.8)$$

But

$$a^0 = a',$$

since

$$k_{\mu} a^{\mu} = 0 = k_0 a^0 + k_1 a^1 = k a^0 - k a^1. \quad (6.9)$$

Similarly

$$b^0 = b'. \quad (6.10)$$

Therefore

$$a^{\mu} b^{\mu} = a^{\mu} b^{\mu}. \quad (6.11)$$

Thus

$$\sum_{\text{pol}} \epsilon_{\mu} a^{\mu} \epsilon_{\nu} b^{\nu} = - a^{\mu} b_{\mu}. \quad (6.12)$$

Then

$$\sum_{\text{pol}} |M_{\mu} \epsilon^{\mu}|^2 = - M^{\mu} M_{\mu} = - M_{\text{e.m.}}^2 T^2, \quad (6.13)$$

where $M_{\text{e.m.}}$ is the electromagnetic interaction expressed

in Equation (6.1). If one takes the average over the nucleon polarizations, T^2 then is written as

$$\frac{1}{4} \sum |U_f T U_i|^2 = \frac{1}{4} \sum |T_{fi}|^2 \quad (6.14)$$

where U_i is the initial nucleon state, U_f is the scattered nucleon state, and T is now the strong interaction between nucleons.

Applying this result to Equation (6.1), one obtains

$$\begin{aligned} \sum_{\text{pol}} |M_{fi}|^2 &= - \left\{ \frac{P_\pi^2}{(P_\pi k)^2} + \frac{P_p^2}{(P_p k)^2} - 2 \frac{P_\pi P_p}{(P_\pi k)(P_p k)} \right\} e^2 \\ &\times \frac{1}{4} \sum |T_{fi}|^2. \end{aligned} \quad (6.15)$$

More explicitly

$$\begin{aligned} \sum_{\text{pol}} |M_{fi}|^2 &= - \left\{ \frac{m_\pi^2}{k^2 (\vec{E}_\pi - \vec{p}_\pi \cdot \vec{n})^2} + \frac{m_p^2}{k^2 (\vec{E}_p - \vec{p}_p \cdot \vec{n})^2} \right. \\ &\quad \left. - 2 \frac{E_\pi E_p - \vec{p}_\pi \cdot \vec{p}_p}{k^2 (\vec{E}_\pi - \vec{p}_\pi \cdot \vec{n})(\vec{E}_p - \vec{p}_p \cdot \vec{n})} \right\} \frac{e^2}{4} \sum |T_{fi}|^2 \end{aligned} \quad (6.16)$$

where $\vec{n} = \vec{k}/k$, and \vec{p}_p is the momentum of the incident proton.

For the elastic case

$$\sum_{\text{pol}} |M_{fi}^{\text{el}}|^2 = \frac{1}{4} \sum |U_f T U_i|^2 = \frac{1}{4} \sum |T_{fi}|^2. \quad (6.17)$$

Again we took the average over the initial and final

nucleon polarizations. Thus, U_i is the initial nucleon state, U_f the final nucleon state and T the strong interaction between nucleons.

To get the cross sections, these results are inserted into Equation (3.16) and Equation (3.31), then one obtains

$$\frac{d^3\sigma}{d\Omega_\pi dE_\pi d\Omega_k} = \frac{m_p m_d P_\pi e^2}{4(2\pi)^5 P_p \{ \vec{n} \cdot (\vec{P}_p - \vec{P}_\pi) - (E_p + m_p - E_\pi) \}} \times \frac{1}{k} \left\{ \frac{2(E_\pi E_p - \vec{P}_\pi \cdot \vec{P}_p)}{(E_\pi - \vec{P}_\pi \cdot \vec{n})(E_p - \vec{P}_p \cdot \vec{n})} - \frac{m_\pi^2}{(E_\pi - \vec{P}_\pi \cdot \vec{n})^2} - \frac{m_p^2}{(E_p - \vec{P}_p \cdot \vec{n})^2} \right\} \times \frac{1}{4} \sum |T_{fi}|^2, \quad (6.18)$$

and

$$\frac{d\sigma^{el}}{d\Omega} = \frac{m_p m_d P_\pi^3}{(2\pi)^2 2P_d \{ \vec{P}_\pi \cdot \vec{P}_p E_\pi - P_\pi^2 (E_p + m_p) \}} \times \frac{1}{4} \sum |T_{fi}|^2. \quad (6.19)$$

Equation (6.18) gives the cross section for $pp \rightarrow \pi d\gamma$, and Equation (6.19) for $pp \rightarrow \pi d$.

One may integrate over a large region by successively adding the contribution from each interval. The pion

CHAPTER 7

NUMERICAL CALCULATION AND DISCUSSION

To obtain

$$\frac{d^3\sigma}{d\Omega_\pi dE_\pi},$$

the integration was carried out with respect to the photon angles Θ_k and φ_k . The calculation was done numerically by using Simpson's rule for double integration. The integration of $f(x)$ between a and $a + 2d$ is given approximately by

$$\int_a^{a+2d} f(x) dx = \frac{d}{3} \{ f(a) + 4f(a+d) + f(a+2d) \}. \quad (7.1)$$

For the double integration, the same process is repeated with respect to the other coordinate to obtain

$$\begin{aligned} \int_a^{a+2d} \int_b^{b+2d} f(x,y) dx dy &= \frac{d^2}{3^2} \{ \{ f(a,b) + 4f(a,b+d) + f(a,b+2d) \} \\ &+ 4 \{ f(a+d,b) + 4f(a+d,b+d) + f(a+d,b+2d) \} \\ &+ \{ f(a+2d,b) + 4f(a+2d,b+d) + f(a+2d,b+2d) \} \}. \end{aligned} \quad (7.2)$$

One may integrate over a large region by successively adding the contribution from each interval. The pion

angle was chosen to be 1°, 20° and 40° in the Laboratory frame, since experimental data at these angles were available. The pion energy was chosen a few MeV lower than that of the elastic value. By using Equation (6.18) and Equation (6.19), one obtains $d\sigma/d\Omega_\pi dE_\pi d\Omega_k$ in terms of $d\sigma^{el}/d\Omega_\pi$, and the only input is the elastic data, i.e. one need not know $(1/4)\sum |T_{fi}|^2$. The elastic data was obtained from the work of Richard-Serre et al (1970). Numerical results were obtained for proton energies equal to 300, 350 and 400 MeV, since this is the range of experimental interest.

The results are shown in the following figures. As can be seen, the radiative tail for the process $pp \rightarrow \pi^+d$ is not very large near threshold. For example, for 300 MeV protons at 1° pion angle, it is in the order of 10^{-3} $\mu\text{b}/\text{MeV}\cdot\text{Ster}$ at 2 MeV below the deuteron peak, while the pion spectrum from the process $pp \rightarrow \pi pn$ has typical values of 1 $\mu\text{b}/\text{MeV}\cdot\text{Ster}$ (Figure 1.1) (Richard-Serre et al 1970).

As mentioned before, one reason for looking at the pion spectrum with high resolution is to search for a well-defined peak that corresponds to the 1S_0 state of the pn system. This state might be difficult to find if

the background from other processes is very large. The results of our calculation, however, show that the contribution from the process $pp \rightarrow \pi^+d\gamma$ to the pion spectrum is not very significant in this energy region. Physically, the reason for this seems to be that the velocity of the scattered pion is too small to emit a significant number of photons. At higher energies, where the pion velocity is higher, one would then expect photon emission to be higher. This is in fact verified by our calculation at proton energy of 600 MeV, (Figure 6.10, 6.11, 6.12), where the result is roughly 15% of the maximum value of the $pp \rightarrow \pi^+pn$ spectrum shown in Figure (1.1)

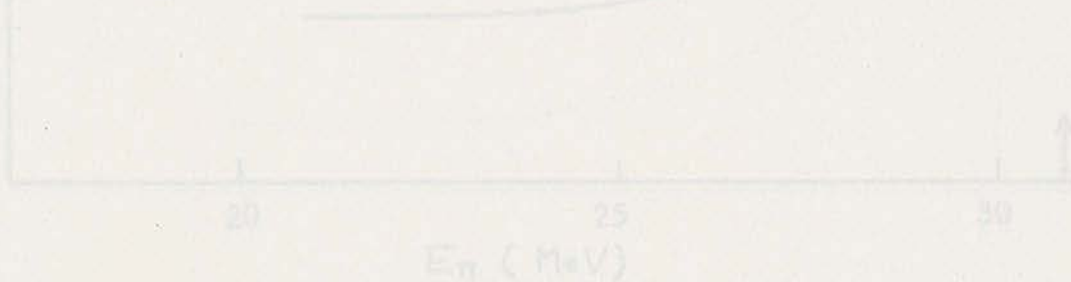


Figure 7.1 Radiative tail from the process $pp \rightarrow \pi^+d$ for 100 MeV protons at a pion angle of 1° . The arrow shows the position of the deuteron peak.

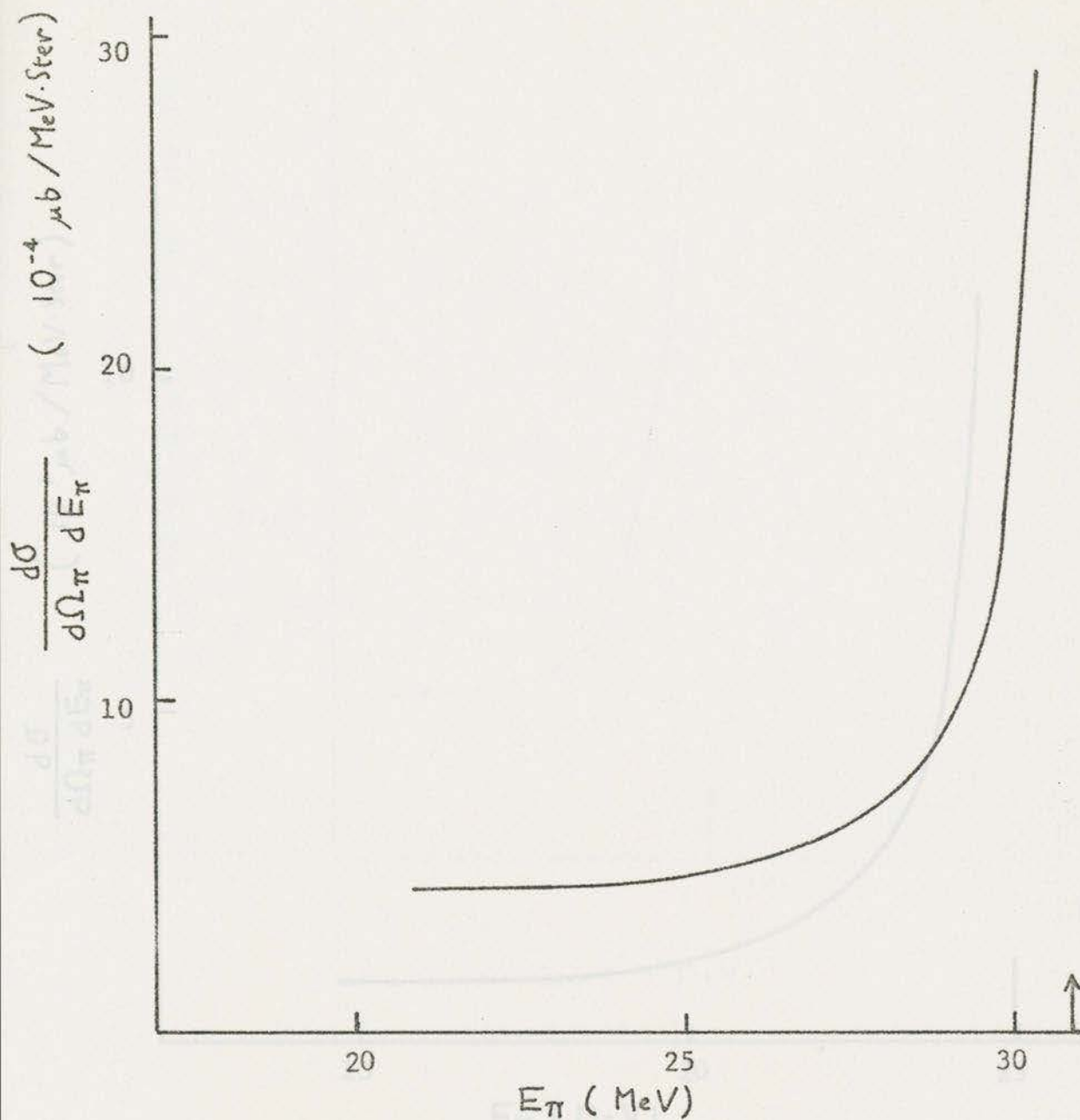


Figure 7.1 Radiative tail from the process $pp \rightarrow \pi^+d$ for 300 MeV protons at a pion angle of 1° . The arrow shows the position of the deuteron peak.

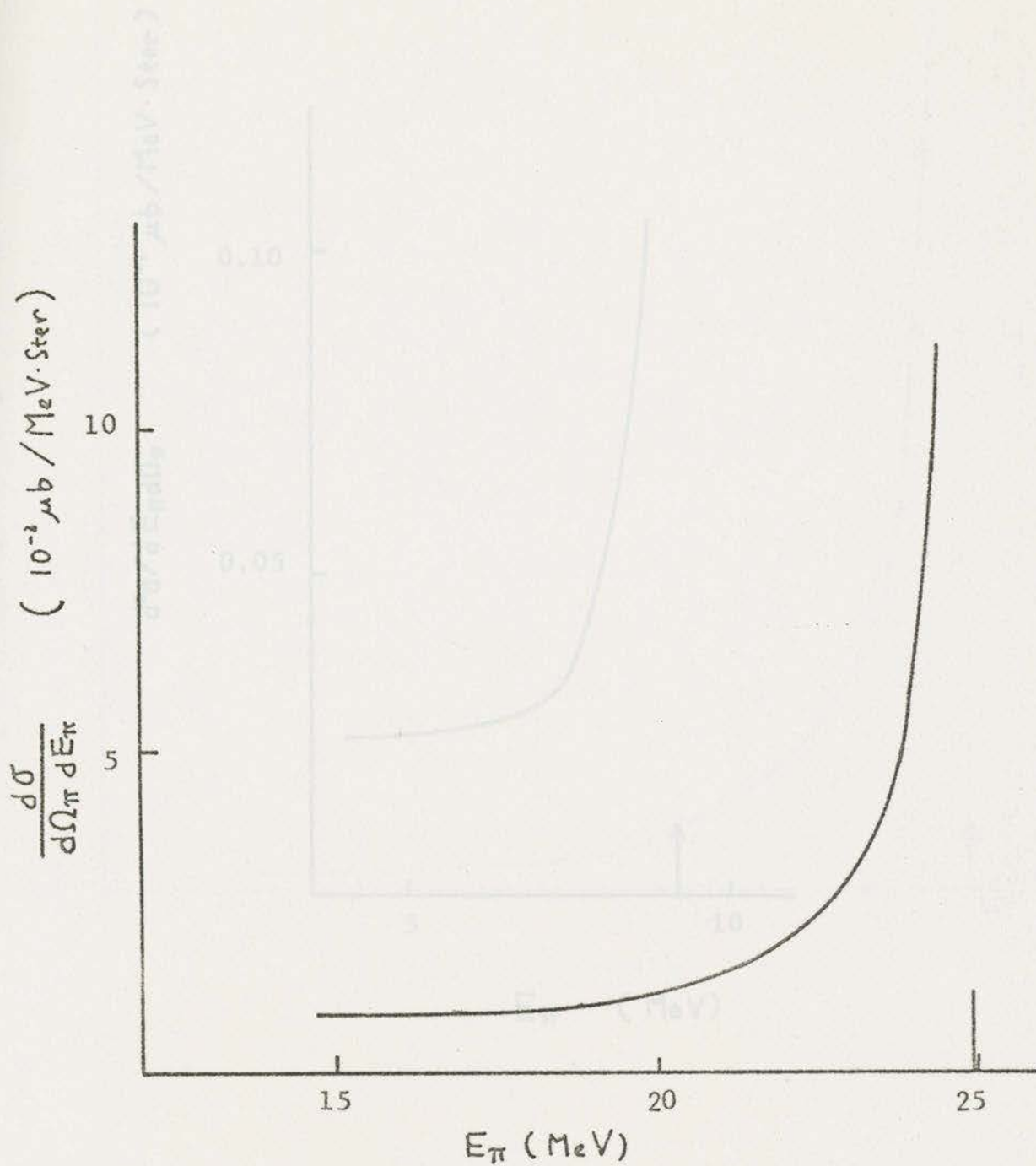


Figure 7.2 Radiative tail from the process $pp \rightarrow \pi^+d$ for 300 MeV protons at a pion angle of 20°

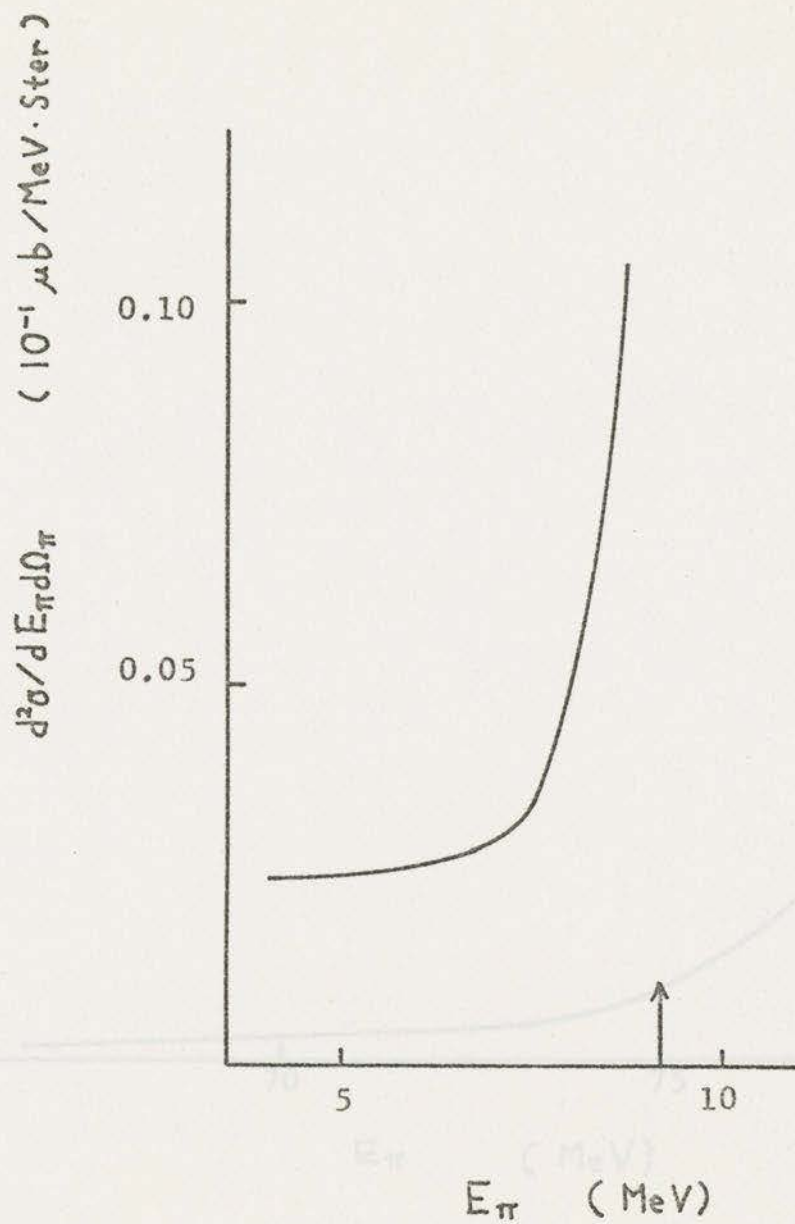


Figure 7.3 Radiative tail from the process $pp \rightarrow \pi^+d$ for 300 MeV protons at a pion angle of 40°

$d^2\sigma/dE_\pi d\Omega_\pi$ (10^{-11} $\mu\text{b}/\text{MeV}\text{-Ster}$)

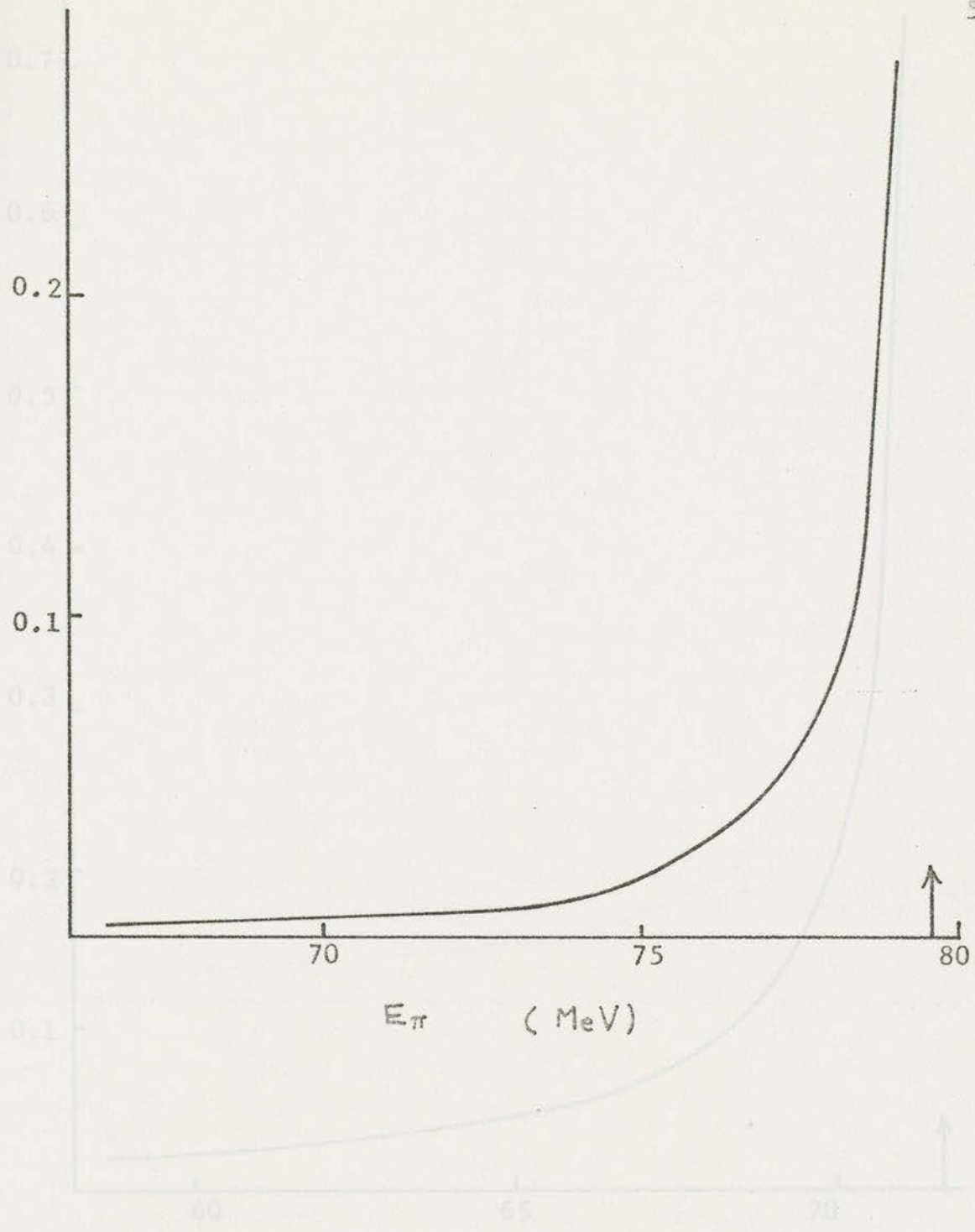


Figure 7.4 Radiative tail from the process $pp \rightarrow \pi^+ d$ for 350 MeV protons at a pion angle of 1°

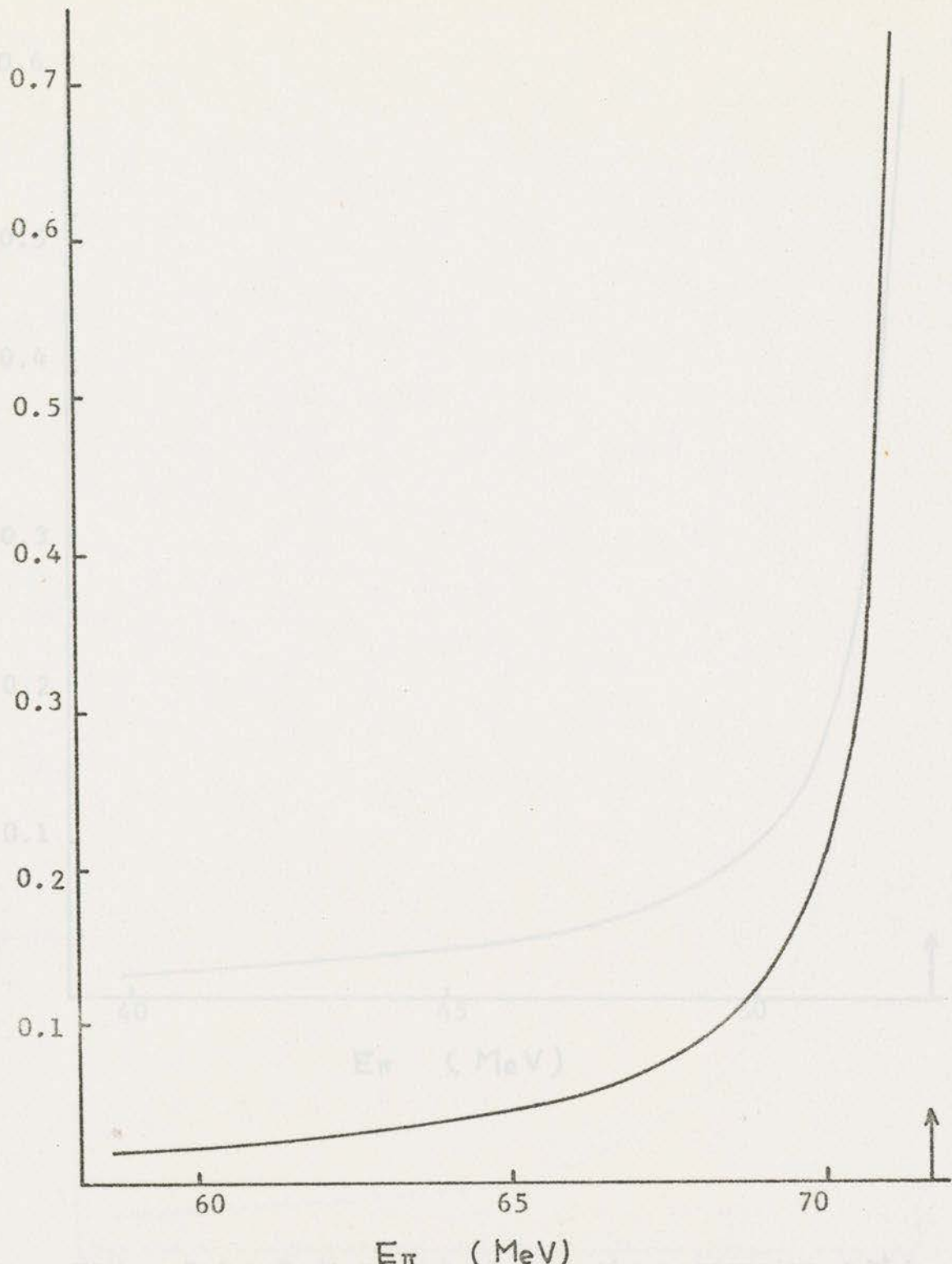


Figure 7.5 Radiative tail from the process $pp \rightarrow \pi^+d$ for 350 MeV protons at a pion angle of 20°

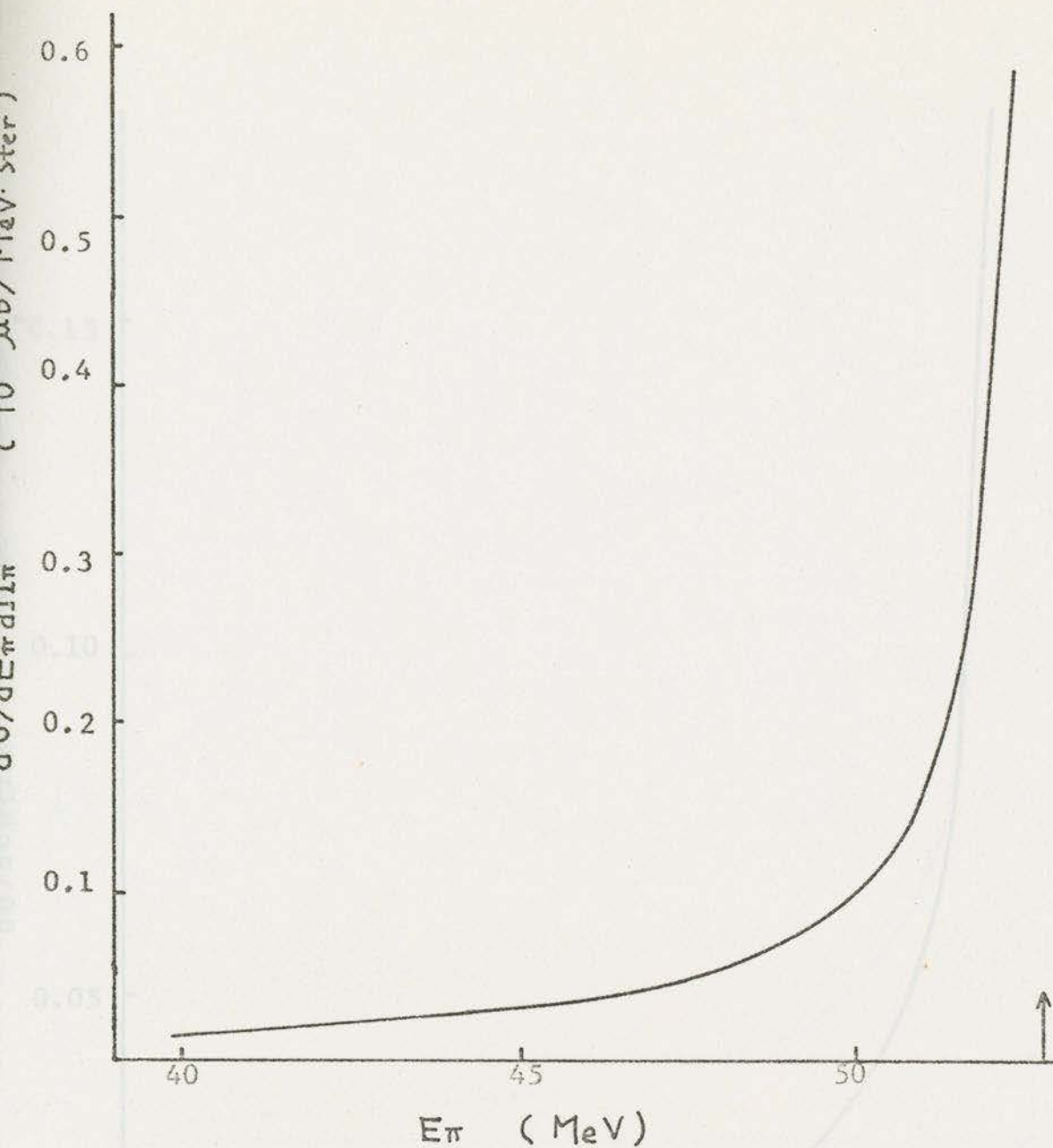


Figure 7.6 Radiative tail from the process $pp \rightarrow \pi^+ d$ for 350 MeV protons at a pion angle of 40°

Figure 7.7 Radiative tail from the process $pp \rightarrow n^+ d$ for 400 MeV protons at a pion angle of 1°

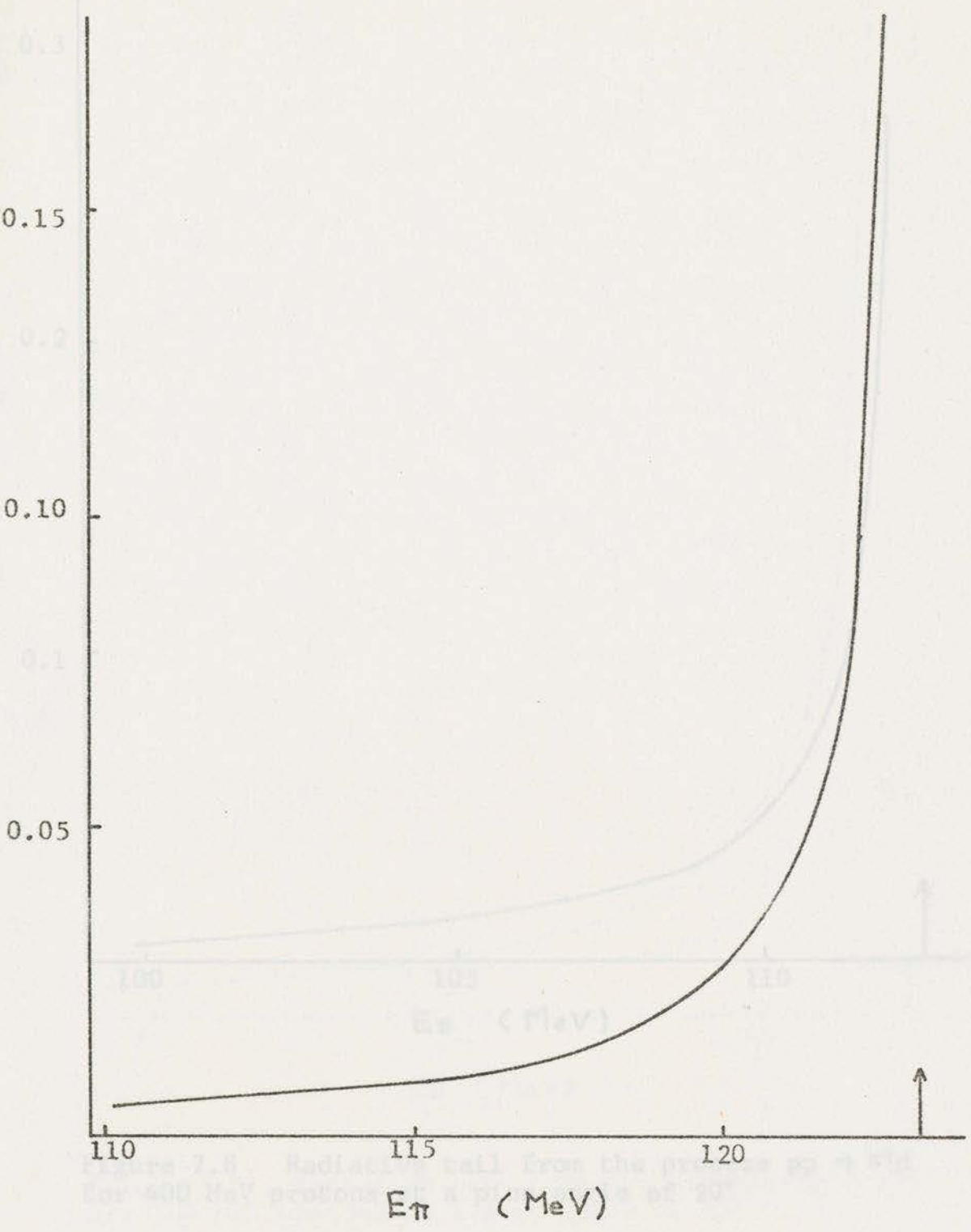


Figure 7.7 Radiative tail from the process $pp \rightarrow \pi^+d$ for 400 MeV protons at a pion angle of 1°

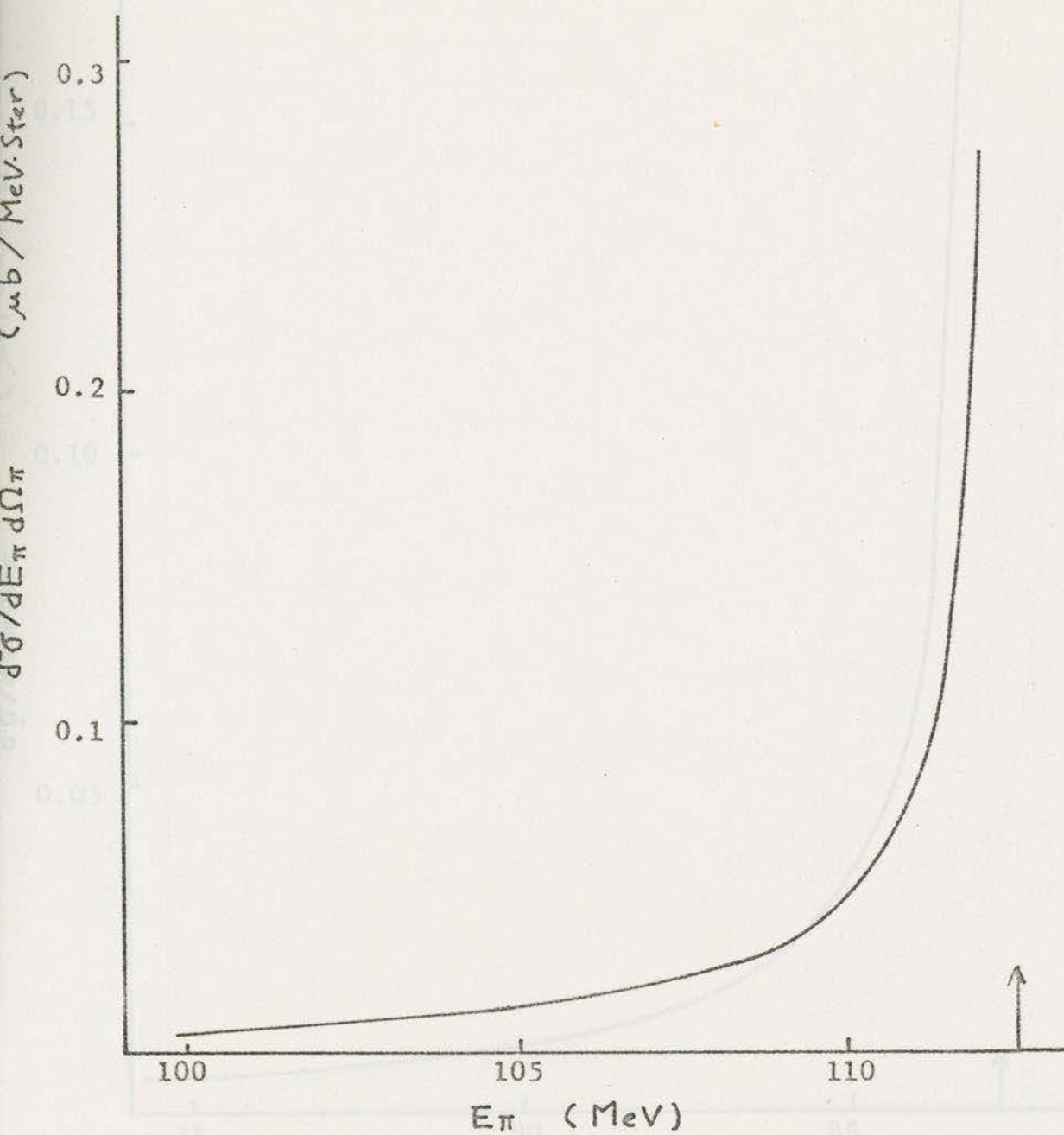


Figure 7.8 Radiative tail from the process $pp \rightarrow \pi^+d$ for 400 MeV protons at a pion angle of 20°

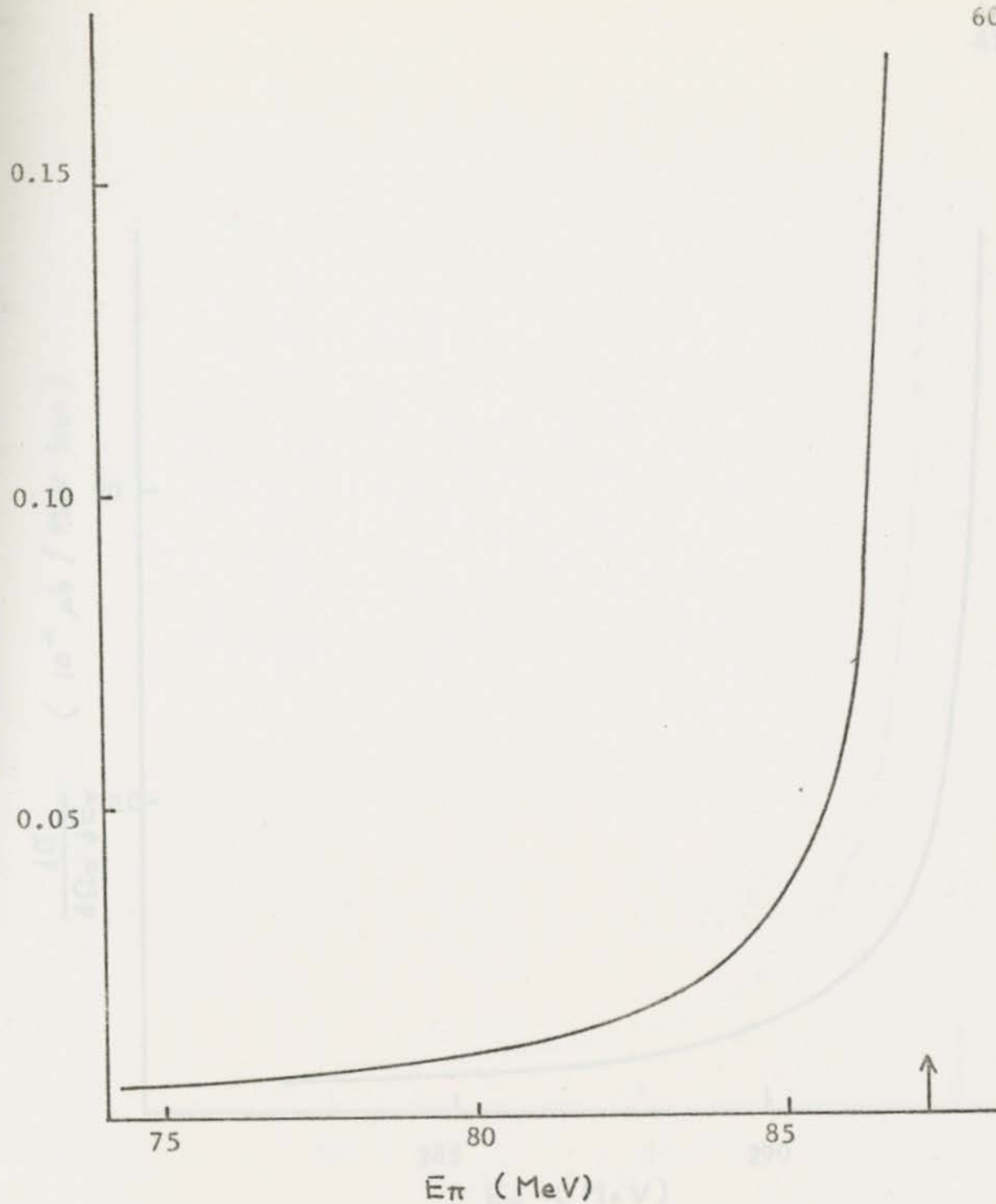


Figure 7.9 Radiative tail from the process $pp \rightarrow \pi^+d$ for 400 MeV protons at a pion angle of 40°

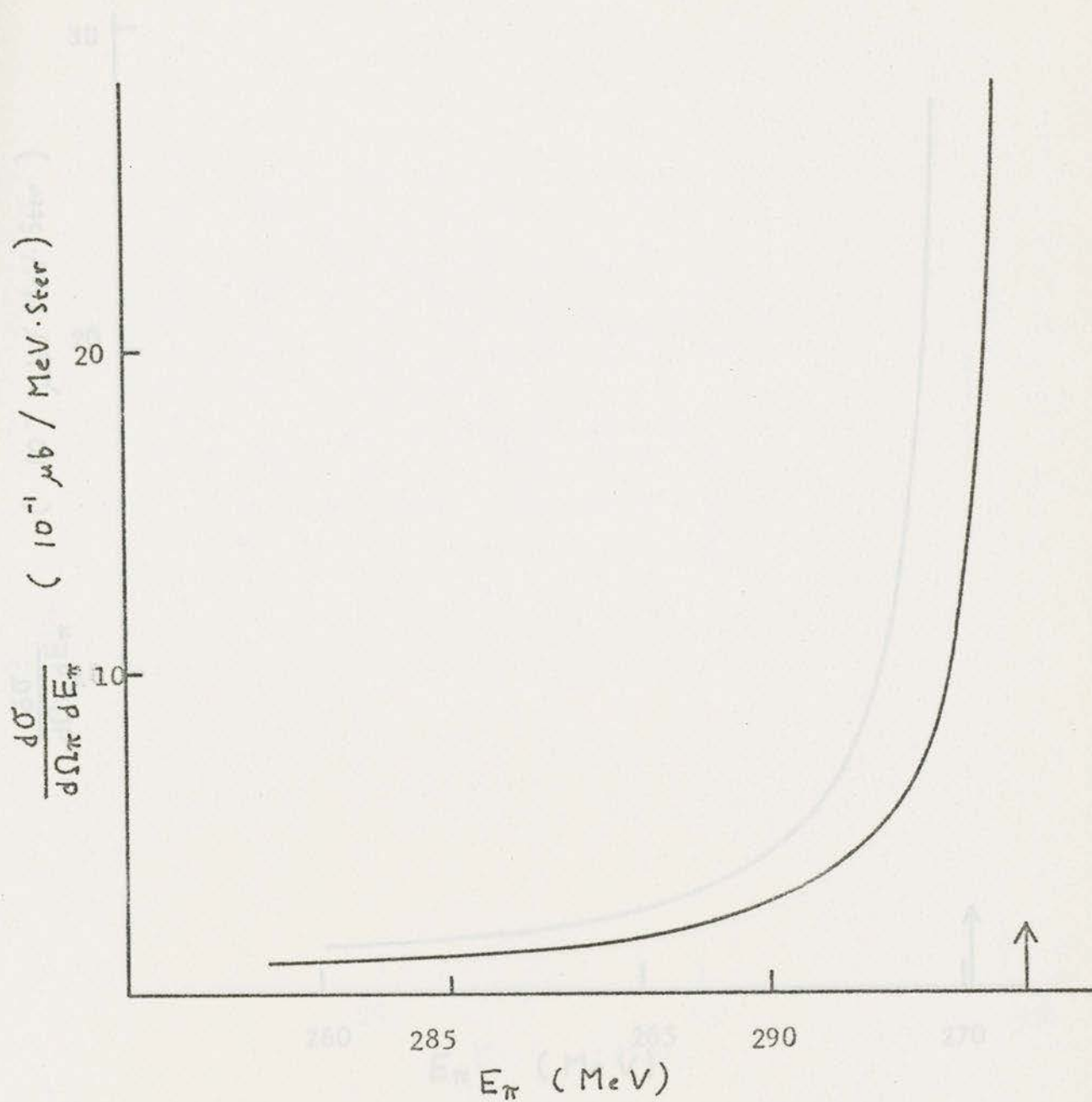


Figure 7.10 Radiative tail from the process $pp \rightarrow \pi^+d$ for 600 MeV protons at a pion angle of 1°

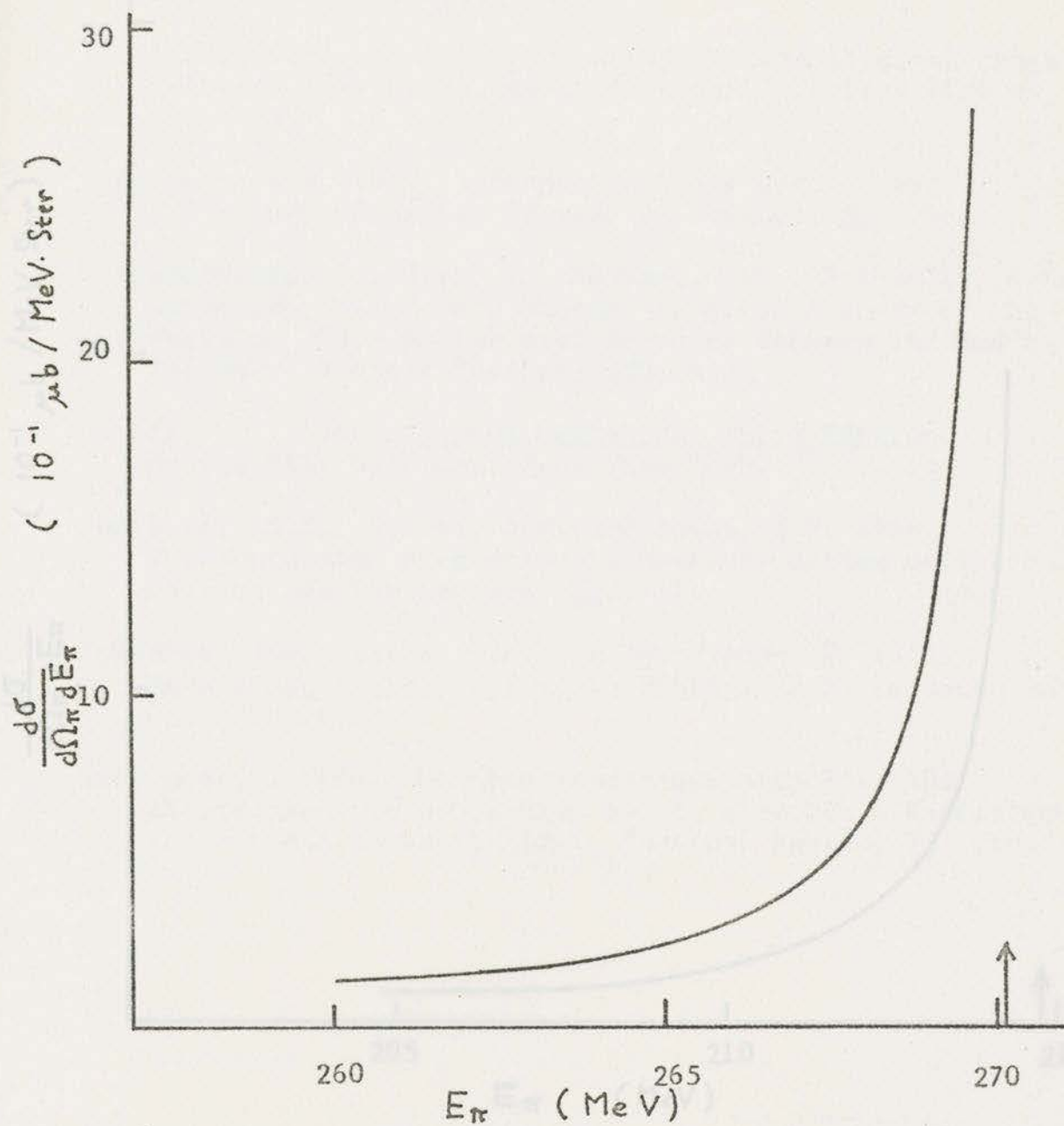


Figure 7.11 Radiative tail from the process $pp \rightarrow \pi^+ d$ for 600 MeV protons at a pion angle of 20°

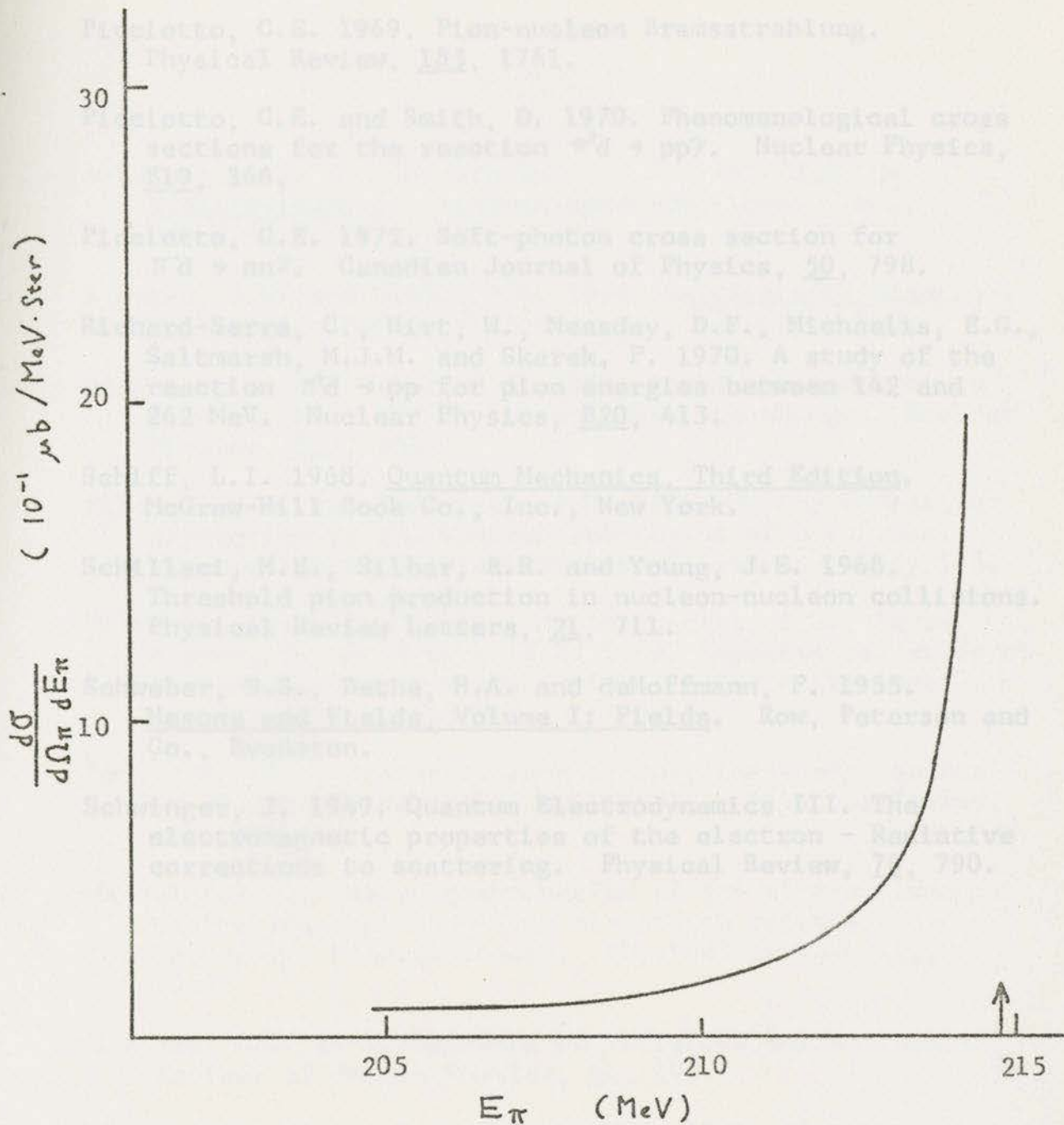


Figure 7.12 Radiative tail from the process $pp \rightarrow \pi^+ d$ for 600 MeV protons at a pion angle of 40°

REFERENCES

- Akheizer, A.J. and Berestetskii, V.B. 1965. Quantum Electrodynamics. Interscience Publishers, Inc., New York.
- Bjorken, J.D. and Drell, S.D. 1964. Relativistic Quantum Mechanics. McGraw-Hill Book Co., Inc., New York.
- Drechsel, D. and Weber, H.J. 1970. Resonance and nucleon pole for $NN \rightarrow NN\pi$ at low and moderate energy. Nuclear Physics, B25, 159.
- Elton, L.R.B. and Robertson, H.H. 1952. On the radiative correction to the Coulomb scattering of electrons. Proceedings of Physical Society (London), A65, 145.
- Hirt, W., Heer, E., Martin, M., Michaelis, E.G., Serre, C., Sharek, P. and Wright, B.T. 1969. Experimental study of the production of charged pions in the collisions protons-core at 600 MeV. CERN69-24.
- Low, F.E. 1958. Bremsstrahlung of very low-energy quanta in elementary particles collisions. Physical Review, 110, 974.
- Mandelstam, S. 1958. Determination of the pion-nucleon scattering amplitude from dispersion relations and unitarity. General theory. Physical Review, 112, 1344.
- Maximon, L.C. 1969. Comments on radiative corrections. Reviews of Modern Physics, 41, 193.
- Motz, J.W., Olsen, H. and Koch, H.W. 1964. Electron scattering without atomic or nuclear excitation. Reviews of Modern Physics, 36, 881.
- Paul, E.B. 1969. Nuclear and Particle Physics. North-Holland Publishing Co., Amsterdam.

- Picciotto, C.E. 1969. Pion-nucleon Bremsstrahlung. *Physical Review*, 185, 1761.
- Picciotto, C.E. and Smith, D. 1970. Phenomenological cross sections for the reaction $\pi^+d \rightarrow pp\gamma$. *Nuclear Physics*, B19, 366.
- Picciotto, C.E. 1972. Soft-photon cross section for $\pi^+d \rightarrow nn\gamma$. *Canadian Journal of Physics*, 50, 798.
- Richard-Serre, C., Hirt, W., Measday, D.F., Michaelis, E.G., Saltmarsh, M.J.M. and Skarek, P. 1970. A study of the reaction $\pi^+d \rightarrow pp$ for pion energies between 142 and 262 MeV. *Nuclear Physics*, B20, 413.
- Schiff, L.I. 1968. Quantum Mechanics, Third Edition. McGraw-Hill Book Co., Inc., New York.
- Schillaci, M.E., Silbar, R.R. and Young, J.E. 1968. Threshold pion production in nucleon-nucleon collisions. *Physical Review Letters*, 21, 711.
- Schweber, S.S., Bethe, H.A. and deHoffmann, F. 1955. Mesons and Fields, Volume I: Fields. Row, Peterson and Co., Evanston.
- Schwinger, J. 1949. Quantum Electrodynamics III. The electromagnetic properties of the electron - Radiative corrections to scattering. *Physical Review*, 76, 790.
- Mandelstam, S. 1958. Determination of the pion-nucleon scattering amplitude from dispersion relations and unitarity. General theory. *Physical Review*, 112, 1344.
- Moravcsik, L.S. 1969. Comments on radiative corrections. *Reviews of Modern Physics*, 41, 193.
- Moft, J.W., Maas, H. and Koch, R.W. 1964. Electron scattering without atomic or nuclear excitation. *Reviews of Modern Physics*, 36, 841.
- Paul, E.B. 1969. Nuclear and Particle Physics. North Holland Publishing Co., Amsterdam.

APPENDIX A

COORDINATES AND MOMENTA

The space-time coordinates $(t, x, y, z) = (t, \vec{x})$ are denoted by the contravariant four-vector in natural units ($c = \hbar = 1$)

$$x^\mu \equiv (x^0, x^1, x^2, x^3) \equiv (t, x, y, z) . \quad (\text{A.1})$$

The covariant four-vector x_μ is

$$x_{,\mu} \equiv (x_0, x_1, x_2, x_3) = (t, -x, -y, -z) = g_{\mu\nu} x^\nu \quad (\text{A.2})$$

with

$$g_{\mu\nu} = \begin{pmatrix} 1 & 0 & 0 & 0 \\ 0 & -1 & 0 & 0 \\ 0 & 0 & -1 & 0 \\ 0 & 0 & 0 & -1 \end{pmatrix} . \quad (\text{A.3})$$

Momentum vectors are defined by

$$p^\mu = (E, p_x, p_y, p_z) . \quad (\text{A.4})$$

The momentum operator in coordinate representation is written

$$p^\mu = i \frac{\partial}{\partial x_\mu} = \left(i \frac{\partial}{\partial t}, \frac{1}{i} \vec{\nabla} \right). \quad (\text{A.5})$$

The four-vector potential of the electromagnetic field is defined by

$$\begin{aligned} A^\mu &= (\Phi, \vec{A}) \\ &= g^{\mu\nu} A_\nu, \end{aligned} \quad (\text{A.6})$$

where Φ is the scalar potential and \vec{A} is the vector potential of electromagnetic field.

APPENDIX BTHE γ MATRICES

The γ matrices in the Dirac equation satisfy the anticommutation relations

$$\gamma^\mu \gamma^\nu + \gamma^\nu \gamma^\mu = 2g^{\mu\nu} \quad (\text{B.1})$$

and are expressed in the commonly used representation as

$$\gamma^0 = \begin{pmatrix} 1 & 0 \\ 0 & -1 \end{pmatrix}$$

$$\gamma^i = \begin{pmatrix} 0 & \sigma^i \\ -\sigma^i & 0 \end{pmatrix} \quad (\text{B.2})$$

where $0 = \begin{pmatrix} 0 & 0 \\ 0 & 0 \end{pmatrix}$, $1 = \begin{pmatrix} 1 & 0 \\ 0 & 1 \end{pmatrix}$ and σ^i are the familiar 2×2 Pauli matrices

$$\sigma^1 = \begin{pmatrix} 0 & 1 \\ 1 & 0 \end{pmatrix} \quad \sigma^2 = \begin{pmatrix} 0 & -i \\ i & 0 \end{pmatrix} \quad \sigma^3 = \begin{pmatrix} 1 & 0 \\ 0 & -1 \end{pmatrix}. \quad (\text{B.3})$$

APPENDIX C

COMPUTER PROGRAM

```

CROSS SECTION
  IMPLICIT REAL*8(A-H,P,S-T)
  INTEGER*2 J,R
  DIMENSION PIA1(3),ECROS(3,3)
  COMMON PRE,PIA,PIE
  COMMON PRM,PRP,PIM,PIP,DEM,DEF,DEP,PI
STATEMENT FUNCTION EXPRESSION OF THE DIFFERENTIAL CROSS SECTION MULTIPLIED
BY DSIN WHICH IS THE FACTOR OF SOLID ANGLE, THE INVARIANT AMPLITUDE IS
SET EQUAL TO 1
  CROS(PHAA,PHAB)=4*C*DSIN(PHAA)*E11/(A**2-B)
  PI=3.141592653589793D0
PRENG=INCIDENT PION ENERGY, PIM=PION MASS, DEM=DEUTERON MASS,
PRM=PROTON MASS, PRE=TOTAL PION ENERGY.
  PRENG=300.000
  PIM=139.600
  DEM=1876.09300
  PRM=938.25600
  PRE=PRENG+PRM
VARIOUS PION ANGLES ARE READ IN.
  READ(5,200)(PIA1(I),I=1,3)
200 FORMAT(3D10.1)
THE VALUES OF THE ELASTIC CROSS SECTION ARE READ FROM EXPERIMENTAL
DATA, THE SUFFIX N IS FOR VARIOUS PION ENERGIES, 1 FOR PION ANGLES
  READ(5,201)((ECROS(I,N),I=1,3),N=1,3)
201 FORMAT(6D11.2/3D11.2)
  TRANS=PI/180
  N=0
  1 PRENG=PRE-PRM
  N=N+1
  WRITE(6,100)PRENG
100 FORMAT('0','PROTON ENERGY=',D12.5)
PRP IS PROTON MOMENTUM,
  PRP=DSQRT(PRE**2-PRM**2)
  DO2 I=1,3
PIANG =PION ANGLE USED IN THIS STEP
  PIANG=PIA1(I)
  WRITE(6,101)PIANG
101 FORMAT('0','PION ANGLE=',F7.2,3X,'PION ENERGY',T46,'% OF CROSS SECT
>ION',T76,'CROSS SECTION BY MILLI BARNS')
PIA IS PION ANGLE EXPRESSED BY RADIAN
  PIA=PIANG*TRANS
ELASTIC PION ENERGY IS CALLED
  CALL ELAST(82)
PIP=PION MOMENTUM
  PIP=DSQRT(PIE**2-PIM**2)
EXPRESSION FOR THE ELASTIC CROSS SECTION, WHERE THE INVARIANT
AMPLITUDE IS SET TO 1
  CROS2=(PRM*DEM*PIP**2/((2*PI)**2*2*PRP*(PRP*PIE*DCOS(PIA)-PIP*(PRE
>+PRM)))
CPIE IS THE ELASTIC PION ENERGY
  CPIE=PIE
DPIE IS THE DIFFERENCE FROM THE ELASTIC PION ENERGY
  DPIE=2.5D-1
  DO3 J=1,7
  DPIE=DPIE*2
  PIE=CPIE-DPIE
  IF(DPIE.LT.PI4)GO TO 2
PIP=PION MOMENTUM/2
  PIP=DSQRT(PIE**2-PIM**2)
  A=PRE+PRM-PIE
  B=(PIP*DSIN(PIA))**2+(PRP-PIP*DCOS(PIA))**2+DEM**2
  C=(PRM*DEM*PIP)/(8*PRP*(2*PI)**5)
  E=PRP-PIP*DCOS(PIA)

```

Surname: TANAKA

Given Name: SHIGEH

Place of Birth: SAITAMA, UTSURUGA, JAPAN

Date of Birth:

1 IS THE NUMBER OF INTERVALS

```

M=30
D=PI/M
SUM=.000
Q=M+1
R=2*M+1
KSIGN=1
FX3=-PI*PRP*DCOS(PIA)+PRE*PIE

```

SIMPSON'S METHOD STARTS

```

DO4 K=1,0
KSIGN=-KSIGN
MULK=3+KSIGN
IF(K.EQ.1)MULK=1
IF(K.EQ.0)MULK=1
PHAA=D*(K-1)
FX1=PRE-PRP*DCOS(PHAA)

```

```

LSIGN=1
DO4 L=1,R
LSIGN=-LSIGN
MULL=3+LSIGN
IF(L.EQ.1)MULL=1
IF(L.EQ.R)MULL=1
PHAB=D*(L-1)
F=-PI*DSIN(PHAA)*DCOS(PHAB)*DSIN(PIA)+DCOS(PHAA)*E-A

```

```

FX2=F+FX1+PRM
FI1=4*(PI/137)*(2*FX3/(FX1*FX2)-PI**2/FX2**2-PRM**2/FX1**2)
SUM=SUM+(D**2/9)*MULK*MULL*DABS(CROS(PHAA,PHAB))

```

4 CONTINUE

```

PIENG=PIE-PI
SUM2=SUM/CROS2
TCROS=SUM2*ECROS(1,N)
WRITE(6,102)PIENG,SUM2,TCROS

```

102 FORMAT(' ',I22,D14.7,I46,D14.7,I76,D14.7)

3 CONTINUE

2 CONTINUE

IF(PPENG-350.000)5,5,6

5 PRE=PRE+50.000

GO TO 1

6 STOP

END

SUBROUTINE ELAST(*)

ENERGY OF PION IN ELASTIC CASE

```

IMPLICIT REAL*8(A-H,P,S-T)
COMMON P,E,PIA,PIE
COMMON PRM,PRP,PIM,PIP,DEM,DEE,DEP,PI
A=2*PRE*PRM+2*PRM**2+PI**2-DEM**2
B=4*PRP**2*DCOS(PIA)**2
C=2*(PRM+PRE)
RC=B-C**2
D=A**2+EC*PIM**2
IF(D.LT.0)RETURN1
S=DSORT(B)*DSORT(D)
PIE=(-A*(+S)/RC
PIF1=(-A*(+S)/IC
IF(PIE.LT.PIF1)PIE=PIF1
RETURN
END

```


THE UNIVERSITY OF VICTORIA LIBRARY
 MANUSCRIPT DISSERTATION (or THESIS)
 AUTHORITY TO DISTRIBUTE

AUTHOR: This dissertation may be lent or microfilm copies made available:

- (a) Without restriction [REDACTED]
- (b) With the restriction that, for a period of five years (until) the written approval of the following is required:
 - (1) The Chairman, School of Graduate Studies
 - (2) The Author
 - (3) both the Chairman, School of Graduate Studies, and the Author

BORROWERS: The borrower undertakes, by signing below, to give proper credit for any use made of the dissertation, and to obtain the consent of the author if it is proposed to make extensive quotations, or to reproduce the dissertation in whole or in part.

Signature of Borrower	Address	Date